

PRESSURE-INDUCED INFRARED ABSORPTION OF  
THE FUNDAMENTAL BAND OF HYDROGEN  
IN H<sub>2</sub>-Ne AND H<sub>2</sub>-Kr MIXTURES AT ROOM  
TEMPERATURE

**CENTRE FOR NEWFOUNDLAND STUDIES**

**TOTAL OF 10 PAGES ONLY  
MAY BE XEROXED**

**(Without Author's Permission)**

WAN-FUNG LEE

14330

MEMORIAL UNIVERSITY  
LIBRARY  
SEP 5 1968  
OF NEWFOUNDLAND



© Copyright 1957

Approved for general circulation  
by the Copyright Office on August 14, 1957  
Library of Congress, Washington, D.C.

September, 1957



PRESSURE-INDUCED INFRARED ABSORPTION OF THE FUNDAMENTAL BAND OF HYDROGEN  
IN H<sub>2</sub>-Ne AND H<sub>2</sub>-Kr MIXTURES AT ROOM TEMPERATURE

by

 Wan-Fung Lee, B.Sc.

Submitted in partial fulfilment  
of the requirements for the degree of Master of Science  
Memorial University of Newfoundland

September, 1967



This thesis has been examined and approved by:

Professor R.L. Armstrong, M.A., Ph.D.,  
Department of Physics,  
University of Toronto,

and

Professor D.H. Rendell, M.Sc., Ph.D.,  
Department of Physics,  
Memorial University of Newfoundland.

## CONTENTS

ABSTRACT	iii
<b>I. Introduction</b>	
1.1 Pressure Induced Absorption: Fundamental Band of Gaseous Hydrogen	1
1.2 Brief Outline of the Theory of Pressure Induced Absorption	6
1.3 Other Infrared Absorptions of Hydrogen	6
1.4 Present Investigation	8
<b>II Experimental Technique</b>	
2.1 The Gas Absorption Cell	10
2.2 Spectroscopic Apparatus	12
2.3 Experimental Procedure	13
2.4 Reduction of the Experimental Traces	19
2.5 Calculation of Partial Density of a Foreign Gas in a Binary Mixture	20
<b>III Experimental Results</b>	
3.1 Absorption Profiles	22
3.2 Absorption Coefficients	27
<b>IV Theory and Calculations</b>	
4.1 Theory	34
4.2 Calculations	41
<b>V Analysis of the Absorption Profiles of the Pressure Induced Infrared Fundamental Band of Hydrogen in H<sub>2</sub>-Ne and H<sub>2</sub>-Kr Mixtures</b>	
5.1 Introduction	49

5.2	Previous Work on Band Profiles of Hydrogen	50
	(i) The rotational-translational absorption spectrum of hydrogen	50
	(ii) The pressure-induced fundamental band of hydrogen	51
5.3	Method of Analysis of the Profiles Obtained in the Present Work	
	(i) The composition of the enhancement absorption profiles of the fundamental band of hydrogen in H <sub>2</sub> -Ne and H <sub>2</sub> -Kr mixtures	52
	(ii) Line-Shape used in obtaining synthetic profiles; and analysis of the profiles	55
5.4	Results and Discussion	57
	Acknowledgments	65
	References	66

## ABSTRACT

The pressure-induced infrared absorption of the fundamental band of hydrogen in  $H_2$ -Ne and  $H_2$ -Kr mixtures was studied at room temperature at a path length of 25.8 cm at pressures up to 400 atmospheres for several base pressures of hydrogen. In the absorption profiles of the band in  $H_2$ -Ne mixtures, the O and S lines are very weak and the Q branch shows a pronounced splitting into two well-resolved components  $Q_P$  and  $Q_R$ . In these contours a doublet structure appears in the S(1) line at all pressures studied, while there is an indication of the same in the  $Q_P$  component at low pressures. In the contours in  $H_2$ -Kr mixtures, the O and S lines are much stronger than the corresponding lines in  $H_2$ -Ne mixtures; the splitting of the Q branch is less pronounced; and at higher pressures, there is an indication of the  $Q_Q$  component besides  $Q_P$  and  $Q_R$ . Integrated absorption coefficients were measured and the binary and ternary absorption coefficients were derived for the fundamental band in each of the mixtures studied.

The theory of the exp-4 model (Van Kranendonk, 1958) was used to calculate the binary absorption coefficients of the individual lines of the O and S branches and of the quadrupole parts of the Q branch of the band in these mixtures. The overlap parts of the binary absorption coefficients were then estimated from the experimental values of the total binary absorption coefficients. Similar calculations were made for the same band in pure hydrogen and in binary mixtures of hydrogen

with He, A and  $N_2$  and the corresponding overlap parts were obtained from the experimental data of Hare and Welsh (1958). The values of the overlap parameters  $\lambda$  occurring in the exp-4 model are then obtained for pure hydrogen and for binary mixtures of hydrogen with He, Ne,  $N_2$ , A, and Kr. A linear relation is established between  $\lambda$  and  $\epsilon$ , the parameter in the Lennard-Jones intermolecular potential. This enables one to obtain  $\lambda$  for  $H_2-O_2$  and  $H_2-Xe$  mixtures and thus to predict the binary absorption coefficients for these two mixtures for which no experimental data are available at present.

The enhancement absorption profiles of the band in  $H_2-Ne$  and  $H_2-Kr$  mixtures were analyzed by a computational procedure using "a Boltzmann dispersion line shape with an exponential tail" for each of the thirteen components of the band at room temperature and the half width  $\delta_Q$  (overlap) and  $\delta_S$  (quadrupolar) were obtained in each case. From the peak intensities of the strongest quadrupolar line,  $S(1)$ , of the band in  $H_2-Kr$  mixtures, the first derivative of the quadrupole moment with respect to internuclear distance of the hydrogen molecule (i.e.  $Q'$ ) was obtained as  $0.51 ea_0$ .

CHAPTER 1

INTRODUCTION

1.1 Pressure Induced Absorption: Fundamental Band of Gaseous Hydrogen:

It is well-known that homonuclear diatomic molecules such as hydrogen, deuterium, nitrogen, oxygen, etc., do not possess a permanent electric dipole moment in their static, rotating, and vibrating states and hence they are not expected to exhibit absorption at their rotational and vibrational frequencies. However, during collisions between molecules at high densities of these diatomic gases and in their high density mixtures with foreign gases, infrared absorption can be observed as a result of dipole moments induced by intermolecular forces. This phenomenon is referred to as "pressure induced absorption" or "collision induced absorption".

Absorption induced by intermolecular forces was first observed by Crawford, Welsh and Locke (1949) in liquid and compressed oxygen with a maximum at the vibrational frequency of the  $O_2$  molecule,  $1556\text{ cm}^{-1}$ , and in compressed nitrogen with a similar maximum at the  $N_2$  vibrational frequency,  $2331\text{ cm}^{-1}$ . In this investigation it was observed that the absorption is proportional to the square of the pressure of the gases at all frequencies of the fundamental bands of  $O_2$  and  $N_2$ . On the basis of this pressure dependence of the absorption, Crawford et al (1949) suggested that a symmetric diatomic molecule absorbs during a collision with either a like molecule or a foreign gas molecule. According to Condon's theory (1932), the dipole moment induced in a

molecule by a static electric field gives rise to transitions obeying the Raman rather than the infrared selection rules. Since the polarization of the molecule by a colliding molecule will produce the same effect, Crawford et al (1949) concluded that the intensity distribution for the induced absorption should be given by Raman selection rules for rotation, i.e.,  $\Delta J = -2$  (O branch), 0 (Q branch), and +2 (S branch), where J is the rotational quantum number. The experimental contours of the pressure induced fundamental bands of  $O_2$  and  $N_2$  have been found to obey these selection rules. The pressure induced fundamental band of  $H_2$ , first observed in the pure gas by Welsh, Crawford, and Locke (1949) and later studied in hydrogen-foreign gas mixtures by Crawford, Welsh, MacDonald, and Locke (1950), has also been found to obey Raman selection rules.

The pressure-induced fundamental band of gaseous hydrogen has been the subject of numerous investigations over a variety of experimental conditions at McLennan Laboratory, University of Toronto. The fundamental band was studied in pure hydrogen and in hydrogen-helium, hydrogen-argon, and hydrogen-nitrogen mixtures at pressures up to 1500 atm at temperatures in the range 376°K to 78°K by Chisholm and Welsh (1954) and at pressures up to 5000 atm at room temperature by Hare and Welsh (1958). These authors have determined the binary and ternary absorption coefficients of the band, and studied, in detail, the  $Q_P$ ,  $Q_Q$ , and  $Q_R$  maxima of the Q branch of the experimental contours. They explained the splitting of the Q branch into  $Q_P$  and  $Q_R$  components as due to the participation of the relative kinetic energies of the colliding pairs of molecules

in the absorption process. The  $Q_Q$ ,  $O$  and  $S$  components are believed to be due to molecular quadrupolar interactions of the colliding pairs of molecules while the  $Q_P$  and  $Q_R$  components are due to electron overlap interactions. Gush, Nanassy, and Welsh (1957) investigated the doublet structures in the  $Q_P$  and  $S(1)$  components of the band under various conditions of temperature and pressure and concluded that these structures could be interpreted in terms of the kinetic energy interactions, just as the main components  $Q_P$  and  $Q_R$  of the  $Q$  branch. The absorption profiles of the fundamental band in the pure gas as well as in hydrogen-foreign gas binary mixtures at low pressures, in the temperature range  $300^{\circ}\text{K}$  to  $78^{\circ}\text{K}$  were analyzed by Hunt and Welsh (1964). Recently Watanabe and Welsh (1964, 1965) studied the fundamental band of hydrogen in pure hydrogen and in hydrogen-helium mixtures at much lower pressures in the temperature range  $18^{\circ}\text{K}$  to  $77^{\circ}\text{K}$  and obtained direct spectroscopic evidence of bound states of  $(\text{H}_2)_2$  complexes at low temperatures. The occurrence of the bound states of  $(\text{H}_2)_2$ ,  $\text{H}_2\text{N}_2$ ,  $\text{H}_2\text{A}$ ,  $\text{H}_2\text{Kr}$ , and  $\text{H}_2\text{Xe}$  complexes was also established spectroscopically by a study of the pressure induced fundamental absorption band of hydrogen in gaseous mixtures at a wide temperature range above the normal boiling point of the perturbing gas by Watanabe, Kudian, and Welsh (1965), Kudian, Welsh, and Watanabe (1965) and Kudian and Welsh (1967).

Transitions at room temperature between the rotational levels of the first two vibrational states ( $v=0$  and  $v=1$ ) of the ground electronic state of hydrogen molecules corresponding to the selection rules  $\Delta J = -2, 0, \text{ and } +2$  are shown schematically in Fig. 1. On account of the very small moment of inertia of the hydrogen molecule, wide spacing is possible for the rotational levels and only a few lines in each of the  $O$ ,  $Q$ , and  $S$  branches are expected

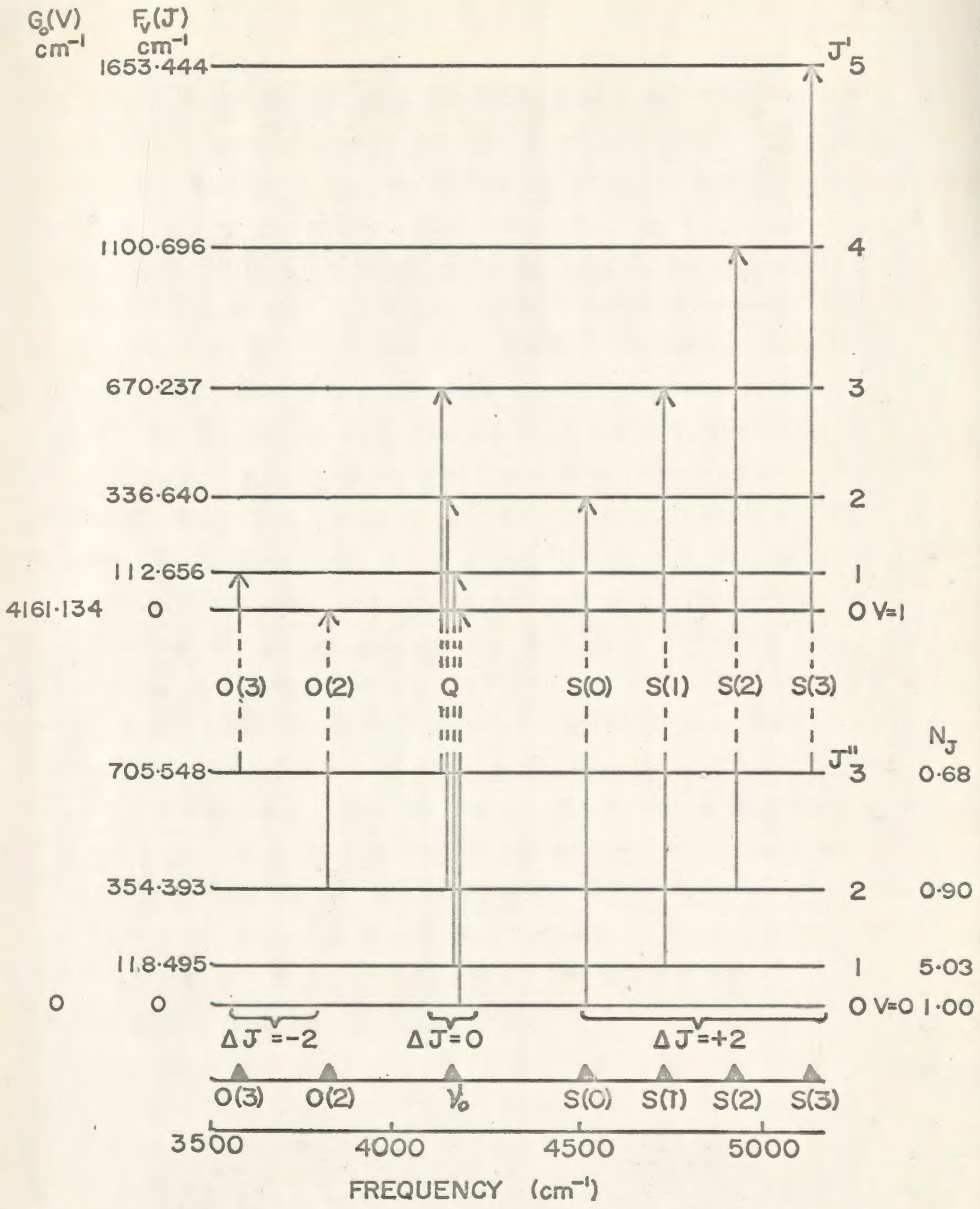


Fig. 1 Energy level diagram of the induced fundamental band of hydrogen.

to occur at room temperature. At low temperatures, even fewer lines are expected. The value of the spectral terms  $G_0(v)$  and  $F_v(J)$  and the positions of the rotational lines are calculated from the molecular constants of hydrogen determined from the high resolution  $R_{\lambda}^a$  spectrum of gaseous hydrogen by Stoicheff (1957) and are shown in the same figure. The relative population,  $N_J$ , of the molecules at room temperature in each of the rotational levels of the ground vibrational state is also shown in the diagram. This was calculated from (i) the Boltzmann distribution law, (ii) the statistical weight of the level arising from the  $(2J+1)$  - fold degeneracy of the rotational levels, and (iii) degeneracy of the level due to nuclear spin. The last factor is calculated as follows: Since the nuclear spin,  $I$ , of a hydrogen atom is  $1/2$ , the total nuclear spin,  $T$ , of a hydrogen molecule takes values 1 (parallel spins) and 0 (antiparallel spins). Even  $T$  values are possible for symmetric levels ( $J=0,2,4,\dots$ ) and odd  $T$  for antisymmetric levels ( $J=1,3,5,\dots$ ). An energy level with a given  $T$  has a statistical weight  $(2T + 1)$  which gives the statistical weight 1, and 3, for the even and odd rotational levels respectively. Since the pressure induced spectra originate from molecular collisions, the individual transitions give rise to very broad lines giving a characteristic broad appearance for the infrared fundamental bands. The fundamental band of hydrogen at room temperature actually extends over more than  $2000 \text{ cm}^{-1}$ .

## 1.2 Brief outline of the Theory of Pressure Induced Absorption

The theory of the pressure induced fundamental band of homonuclear diatomic molecules was given by Van Kranendonk and Bird (1951a, 1951b). Van Kranendonk (1952, 1957, 1958, 1959) and Britton and Crawford (1958). According to Van Kranendonk (1958), the induced dipole moment in a binary collision between an absorbing homonuclear diatomic molecule and a perturbing molecule consists of two additive parts. One part is the short-range electron overlap dipole moment which decreases exponentially with intermolecular distance,  $R$ . The other part is the long-range dipole moment resulting from the polarization of one molecule by the quadrupole field of the other and is proportional to  $R^{-4}$ . According to this "exp-4" model, the dipole moment induced by overlap forces is, to a first approximation, spherically symmetric, i.e. almost independent of the orientation of the molecules and mainly contributes to the intensity of the Q branch; but the long-range dipole moment is strongly dependent on the mutual orientation of the colliding pair and gives rise to transitions in the O, Q and S branches. The above theory of Van Kranendonk has been applied in the interpretation of the experimental bands of hydrogen, deuterium, nitrogen and oxygen in pure gases and in their binary mixtures with foreign gases by various investigators.

## 1.3 Other Infrared Absorptions of Hydrogen

Many interesting features of the fundamental band of hydrogen in the liquid and solid phases were studied experimentally at University of Toronto by Allin, Hare and MacDonald (1955); Allin, Gush, Hare and Welsh (1955); Gush, Hare, Allin and Welsh (1957); Allin, Gush, Hare

and Welsh (1958), Gush, Hare, Allin and Welsh (1960), Gush (1961), and Clouter and Gush (1965). A detailed theoretical treatment of the rotational and vibrational motions of the molecules that are responsible for various features of the band in solid hydrogen was given by Van Kranendonk (1959, 1960), Poll and Van Kranendonk (1962), Gush and Van Kranendonk (1962), Sears and Van Kranendonk (1964), and Van Kranendonk and Sears (1965).

The general features of the infrared induced absorption of dilute solutions of  $H_2$  in liquid argon and in liquid neon were studied by Ewing and Trajmar (1964, 1965).

The pressure induced rotational spectrum of hydrogen which occurs in the far infrared region was observed for the first time by Ketelaar, Colpa, and Hooge (1955). It was studied in more detail in pure hydrogen and in hydrogen-foreign gas mixtures by Colpa and Ketelaar (1958a), Kiss, Gush and Welsh (1959), and Kiss and Welsh (1959). Recently Bosomworth and Gush (1965) studied the absorption of the low frequency wing of the pure rotational spectrum of hydrogen as well as its pure translational absorption spectrum. The pressure-induced rotational absorption spectrum of hydrogen was theoretically treated by Colpa and Ketelaar (1958b) and by Van Kranendonk and Kiss (1959). The theory of translational absorption in gases was given by Poll and Van Kranendonk (1961).

The pressure induced first overtone band of hydrogen was investigated by Welsh, Crawford, MacDonald and Chisholm (1951) and later by Hare and Welsh (1958).

#### 1.4 Present Investigation

The present investigation was designed to obtain new information on the pressure induced fundamental band of hydrogen using neon and krypton as perturbers at room temperature. The band was studied in  $H_2$ -Ne and  $H_2$ -Kr mixtures at a path length of 25.8 cm. at pressures up to 400 atm. using several base pressures of hydrogen. Integrated absorption coefficients were measured and the binary and ternary absorption coefficients were derived for the fundamental band in each of the mixtures studied. Using more recent data of the binary absorption coefficients of the band in  $H_2$ - $H_2$ ,  $H_2$ -He,  $H_2$ -A, and  $H_2$ - $N_2$  mixtures as obtained by Hare and Welsh (1958), and those of this band in  $H_2$ -Ne and  $H_2$ -Kr mixtures obtained in the present investigation, the electron overlap parts and the molecular quadrupole parts of these binary absorption coefficients were separated. The values of the overlap parameter  $\lambda$  occurring in the theory of "exp-4" model of Van Kranendonk (1958) are then obtained for pure hydrogen and for binary mixtures of hydrogen with He, Ne,  $N_2$ , A, and Kr. A new relation is established between  $\lambda$  and  $\epsilon$ , the parameter occurring in the Lennard-Jones intermolecular potential. From this, one obtains  $\lambda$  for the mixtures  $H_2$ - $O_2$  and  $H_2$ -Xe, and can thus predict the binary absorption coefficients of these two mixtures for which no experimental data are available at present. The absorption coefficients of the individual lines of the O and S branches and of the quadrupole parts of the Q branch of the band were calculated for mixtures for which experimental data are available. The enhancement absorption profiles of the band in  $H_2$ -Ne

and H<sub>2</sub>-Kr mixtures were analyzed by a computational procedure using "a Boltzmann dispersion line shape with an exponential tail" for each of the thirteen components of the band at room temperature and the half-widths  $\delta_Q$  (overlap) and  $\delta_S$  (quadrupolar) were obtained in each case. From the peak intensities of the strongest quadrupolar line, S(1), of the band in H<sub>2</sub>-Kr mixtures, the first derivative of the quadrupole moment with respect to internuclear distance of the hydrogen molecule (i.e.  $Q^1$ ) was obtained as  $0.51 e a_0$ .

CHAPTER 2

EXPERIMENTAL TECHNIQUE

In this chapter a description of the apparatus used, and the experimental procedure adopted, in the study of the pressure-induced fundamental band of hydrogen in H<sub>2</sub>-Ne and H<sub>2</sub>-Kr mixtures compressed at pressures up to 7000 p.s.i. at room temperature, is given.

2.1 The Gas Absorption Cell

A section of the 25.8 cm. transmission type absorption cell used in the present investigation is shown in Fig. 2. Its constructional details were described by Sinha (1967). The cell mainly consists of the cell body A, 15.5 in. long and 3.2 in. in diameter with a central bore of 3/4 in., and was made of stainless steel of type no. 303. A stainless steel light guide, G, made in two sections and having a central rectangular aperture, 3/8 in. x 3/16 in., was inserted into the central bore. The inside surface of the light guide was polished to ensure a good reflection of radiation. Both the entrance and exit windows, W, were polished synthetic sapphire plates 1 in. in diameter and 5 mm. thick. They were sealed on to the optically flat stainless steel window plates, P, with a thin layer of General Electric silicone rubber cement. Stainless steel retaining caps, C, held the windows in place when the cell was evacuated; teflon washer, D, placed between the cap and the window prevented chipping of the window when the cap was tightened. The dimensions of the rectangular apertures in the window plates were the same as those of the apertures of the light

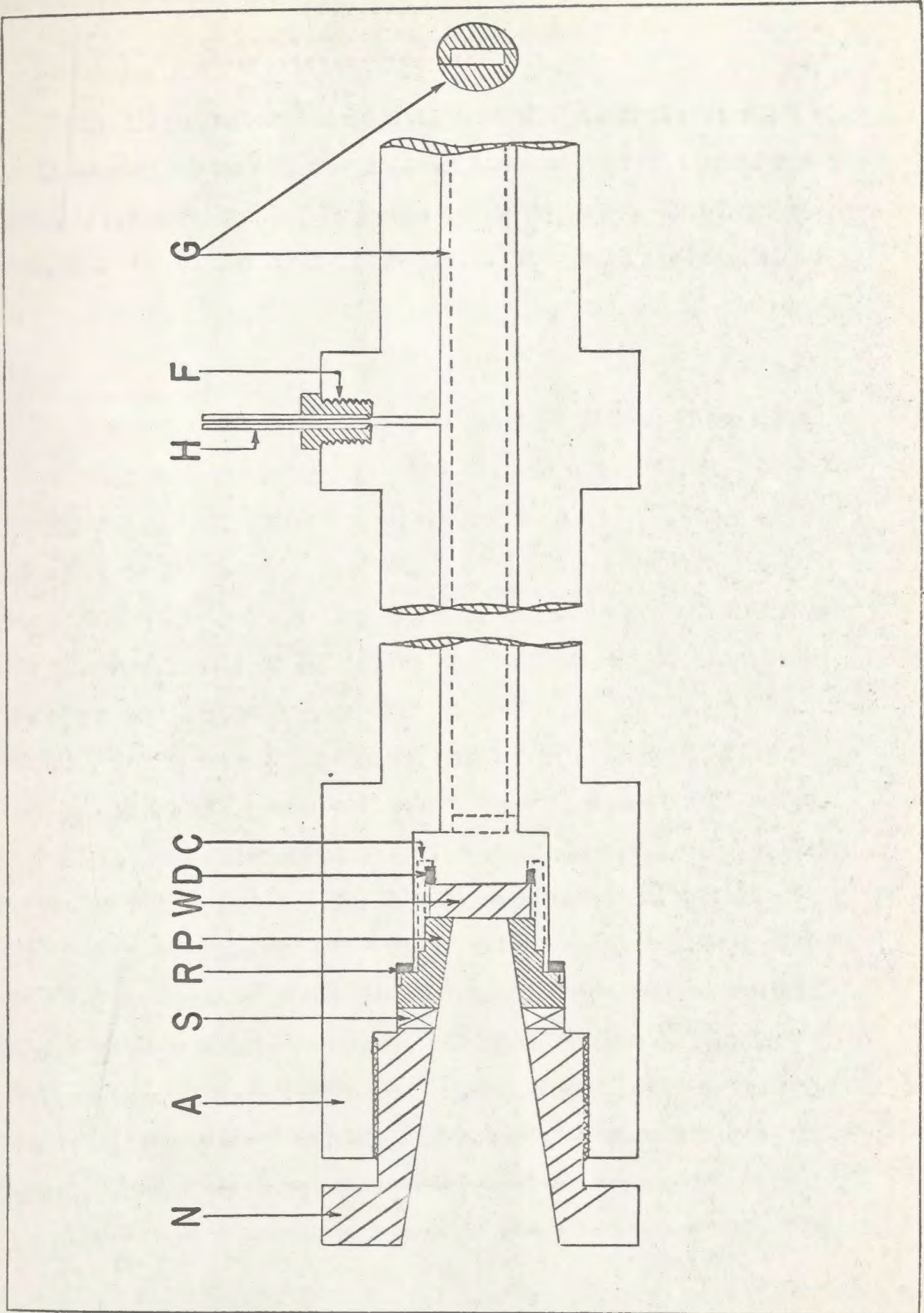


Fig 2. High pressure gas absorption cell

guide. The apertures of the assembled cell were designed to allow a  $f/4$  cone of radiation to focus the source and the spectrometer slit onto the entrance and exit ends of the cell respectively. A very good pressure seal was obtained by using invar rings, R, 1/8 in. thick, between the window plates, P, and the body of the cell. To prevent non-alignment of the light guide and the apertures of the window plates, the portion, S, of the window plates was designed to be square in shape, 0.35 in. in thickness, to fit exactly into a matched square recess in the cell body. The hexagonal stainless steel closing nuts, N, were tightened to hold the cell pressure-tight. A steel capillary tube, H, 1/4 in. in diameter served as the gas inlet to the cell and was connected to the cell by means of an Aminco-fitting, F. The cell was tested by Sinha for pressures up to 1200 atm at room temperature and up to 400 atm, at liquid nitrogen temperature. The absorption path length was measured by subtracting the length of two sapphire end plates from the total length of the assembled cell.

## 2.2 Spectroscopic Apparatus

The experiments in the present investigation were performed with a Perkin-Elmer Model 112 double pass spectrometer using a LiF prism and a PbS detector (Kodak "Ektron" type N cell). The infrared source was a General Electric 750 watt tungsten filament projection lamp operated at 2.6 amps and 24 volts obtained from a stabilized semiconductor d.c. power supply unit, Model RVC 35-5, supplied by NJE Corporation, New Jersey, which was fed by a Sorenson A.C. regulator, Model ACR-2000.

The entire optical arrangement used with the absorption cell, H, is shown in Fig. 3. Radiation from the source, S, was focused on the entrance window of the cell by means of an aluminized spherical front surface mirror,  $M_1$ , having a radius of curvature, 15.9 in. After traversing the cell, the radiation from the exit window was reflected and focused onto slit  $S_1$ , of the spectrometer, A, with the help of a second spherical mirror,  $M_2$ , which was identical to  $M_1$ . A F/4 light cone was used in the external optical system with each of the mirrors  $M_1$  and  $M_2$  in order to match the internal optics of the spectrometer.

A frequency calibration for the spectrometer in the region of the pressure-induced fundamental band of hydrogen i.e. from  $3500 \text{ cm}^{-1}$  to  $5800 \text{ cm}^{-1}$ , was obtained using the known frequencies of the absorption peaks of the atmospheric water vapor (Perkin-Elmer spectrometer instruction manual, Vol. 3A), liquid <sup>n</sup>idene (I.U.P.A.C. Tables of Wavenumbers, 1961) and 1,2,4-trichlorobenzene (Plyler and Acquista, 1952). The spectrometer slit width was maintained at  $100\mu$ , which gave a spectral resolution of  $\sim 9 \text{ cm}^{-1}$  at  $4161 \text{ cm}^{-1}$ , the origin of the fundamental band of hydrogen.

### 2.3 Experimental Procedure

Prior to the actual experiments, the high pressure gas system consisting of a mercury-column gas compressor, an Aminco hand-operated oil pump, Bourdon-type pressure gauges, thermal compressors, absorption cell, Aminco needle valves shown schematically in Fig. 4 was tested for pressure up to 12000 p.s.i. for several days and for vacuum up to  $\sim 0.1 \text{ mm}$  pressure of mercury for several hours.

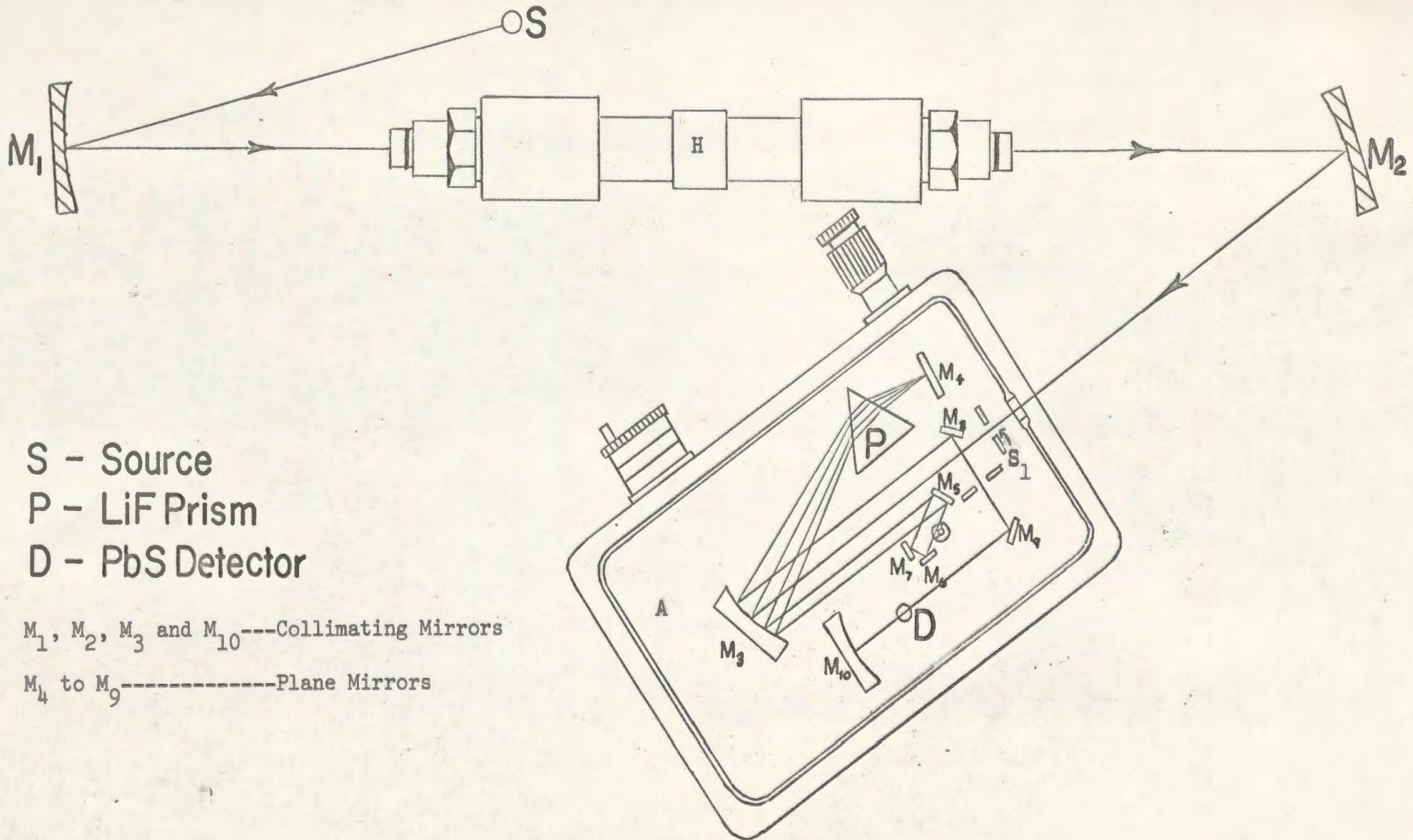


Fig. 3 Top view of the optical components of the experimental set up including Perkin-Elmer Model 112 Spectrometer.

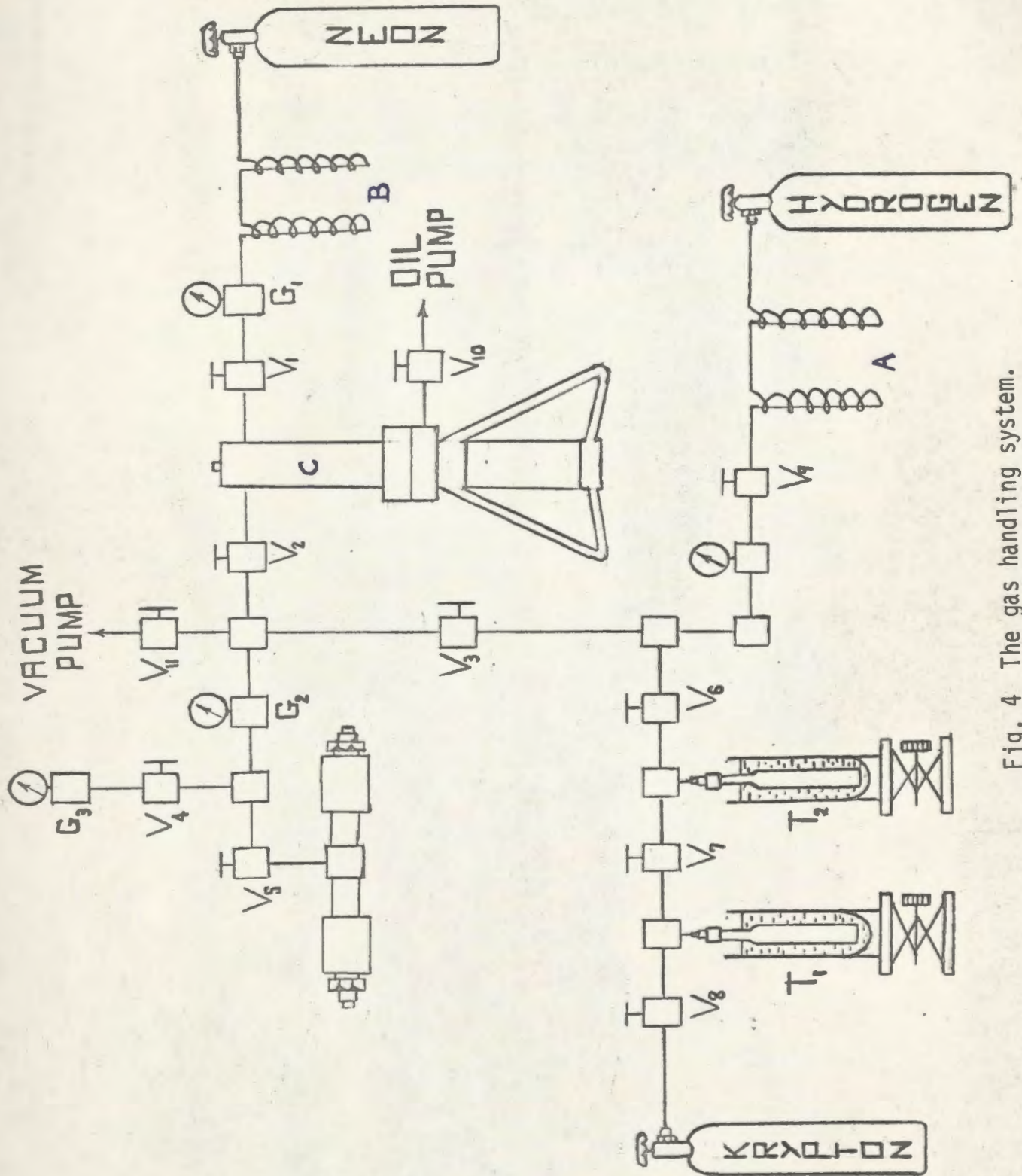


Fig. 4 The gas handling system.

Before an experiment was performed, hydrogen gas was flushed through the system which was then evacuated. This procedure was repeated several times in order to make sure that there was no trace of oxygen left in the system to prevent the possibility of formation of water vapor which might affect the background of the spectrometer traces.

The pressure gauges used in the high pressure system were calibrated by using an Ashcroft dead-weight tester. Different components of the system were connected by stainless steel capillary tubing with 1/4 in. outside diameter. Before the system was assembled, the gas compressors, needle valves, the absorption cell, etc., were thoroughly cleaned with benzene. The length of the capillary tubing connecting the valve  $V_5$  and the absorption cell (Fig. 4) was made as short as possible to minimize the experimental error caused by the amount of the hydrogen present therein. To test the performance of the present experimental set up, the pressure-induced fundamental band of hydrogen in the pure gas was studied. It was found that the binary and ternary absorption coefficients of the band obtained for pure hydrogen agreed very well with those obtained by earlier investigators.

H<sub>2</sub>-Ne Experiments: For each mixture experiment hydrogen gas from a cylinder, after slowly passing through the liquid nitrogen traps A, was admitted into the evacuated absorption cell with valves  $V_2$ ,  $V_6$ , and  $V_{11}$  closed. The base pressure of hydrogen was measured by means of the low range gauge,  $G_3$ , for better accuracy. Absorption spectrum

of pure hydrogen gas was then recorded until a satisfactory reproduction of the spectrometer traces was obtained. Then with valves  $V_5$ ,  $V_4$ ,  $V_2$ ,  $V_6$  and  $V_9$  closed, the system was re-evacuated through the valve,  $V_{11}$ , and isolated by closing the same valve. Neon gas was first purified in liquid nitrogen traps B and then compressed by a column of mercury in the gas compressor C, driven by an Aminco hand-operated oil pump. It was then admitted into the absorption cell at required pressures by using the so-called "pulsating technique" which consisted of opening and closing the valve,  $V_5$ , momentarily three or four times at proper intervals. The pressure reading of the gas mixture inside the cell was read on the gauge  $G_2$  when the final momentary opening of the valve,  $V_5$ , showed no change in pressure. The mixing was assumed to be complete when the deflection of the pen of the recorder, which usually falls off during the sudden introduction of the foreign gas into the absorption cell, regained its original level. For  $H_2$ -Ne mixtures the duration of mixing was  $\sim 15$  minutes. To prevent sudden fluctuation of the mercury level in the gas compressor while admitting compressed neon from the gas compressor into the absorption cell, the valve,  $V_{10}$ , connecting the gas compressor and the oil pump, was closed. For each pressure of the mixture, spectrometer traces were recorded until a satisfactory reproduction was obtained. Several base pressures of hydrogen ranging from 14 atm to 54 atm were used for the experiments with neon as a perturbing gas.

$H_2$ -Kr Experiments: As krypton gas is expensive, a somewhat different arrangement was used for the experiments with  $H_2$ -Kr mixtures so that krypton could be separated from the mixture and saved, after the

necessary experimental traces were obtained. The details of this arrangement are also shown in Fig. 4. The only difference between the experimental procedures for H<sub>2</sub>-Ne and H<sub>2</sub>-Kr mixtures was that two thermal compressors T<sub>1</sub> and T<sub>2</sub> were used, instead of a mercury-column gas compressor, to develop high pressures of krypton; and the same were used to separate krypton from H<sub>2</sub>-Kr mixtures. The actual experimental procedure is as follows: A requisite amount of krypton from a cylinder supplied by Matheson Company of Canada was introduced, through the valve, V<sub>8</sub>, and solidified (freezing point: -156.6°C; boiling point: -152.9°C) in the thermal compressors T<sub>1</sub> and T<sub>2</sub> which were cooled to liquid nitrogen temperature (boiling point: -195.8°C). Moderate pressures of krypton were then obtained from solid krypton, through evaporation, by lowering the level of liquid nitrogen surrounding T<sub>1</sub> after closing the valve, V<sub>8</sub>. To obtain higher pressures, solid krypton in T<sub>2</sub> was evaporated similarly with the valve, V<sub>7</sub>, closed. When an H<sub>2</sub>-Kr mixture experiment was completed, the separation of krypton from the mixture was rather simple because of the large difference in the boiling point of hydrogen (-252.8°C) and the freezing point of krypton. Krypton from the mixture was condensed into the thermal compressors immersed in liquid nitrogen and the uncondensed hydrogen gas was then slowly let out of the system which was evacuated later. Care must be taken to prevent the escape of the powder-like krypton crystals along with hydrogen gas. Evaporation and then condensation of krypton and evacuation of the system were repeated once again. The purity of the collected krypton from the mixture was checked by studying its

spectrum in the hydrogen fundamental band region. When krypton was suddenly introduced into the absorption cell containing a particular pressure of hydrogen, it was found that the deflection of the pen of the recorder decreased considerably and it took 30 to 40 minutes before it regained its original level. It was also noticed that the change in the deflection of the pen on introduction of krypton into the absorption cell depended to some extent, on the pressure of the mixture in the cell. This might be due to the fluctuation of the refractive index of the gases as the pressure was changed. When the partial pressure of krypton in the mixture was high (say  $\sim 250$  atm), krypton in the absorption cell became solidified, due to Joule-Thomson cooling during the expansion, while it was recollected into the thermal compressors.

#### 2.4 Reduction of the Experimental Traces

In the present experiments, the enhancement in absorption by the introduction of a foreign gas at various pressures into the absorption cell containing a particular base pressure of hydrogen was of main interest. Therefore the absorption traces obtained for mixtures for different pressures of the foreign gas in an experiment were plotted on the background trace obtained with a base pressure of hydrogen, after a careful "matching". Water absorption peaks that appeared on both ends of hydrogen fundamental band were used as frequency references. The traces were then reduced by using a standard logarithmic scale that gave  $\log_{10}(I_1/I_2)$  which determined the absorption coefficient  $\alpha_{en}(\nu)$  defined by Beer's law

$$I_2 = I_1 \exp(-\alpha_{en}(\nu)\ell)$$

or

$$\alpha_{en}(\nu) = \frac{2.303}{\ell} \log_{10} \frac{I_1}{I_2}$$

where  $I_1$  is the intensity transmitted by pure hydrogen in the cell of optical path length,  $\ell$ , at a particular frequency  $\nu$  in  $\text{cm}^{-1}$ ,  $I_2$  is the intensity with a binary gas mixture in the cell at the same frequency  $\nu$ , and  $\alpha_{en}(\nu)$  is the corresponding enhancement in the absorption coefficient. The profiles of the enhancement absorption were obtained by plotting  $\log_{10}(I_1/I_2)$  vs. frequency in  $\text{cm}^{-1}$ ,  $\nu$ , at intervals of  $20 \text{ cm}^{-1}$  across the band.

## 2.5 Calculation of Partial Density of a Foreign Gas in a Binary Mixture

The base density of hydrogen,  $\rho_a$ , was directly obtained from the isothermal data given by Michels and Goudekot (1941). Three different bases of hydrogen (37.6, 48.7, and 45.0 Amagat) were used for  $\text{H}_2$ -Ne mixture experiments, and three (12.2, 14.2, and 15.8 Amagat) for  $\text{H}_2$ -Kr mixture experiments. The densities used were expressed in Amagat unit of density, which is defined as the ratio of the density at a given pressure and temperature to the density at N.T.P.

The partial density,  $\rho_b$ , of the foreign gas in a binary gas mixture was determined by using the interpolation formula

$$\rho_b = \frac{1}{1+\beta'} ( (\rho_a)_p + \beta' (\rho_b)_p ) - \rho_a$$

where  $\beta' = \rho_b' / \rho_a$  is the approximate mixture ratio and  $\rho_b'$  is the approximate partial density of the foreign gas which was obtained

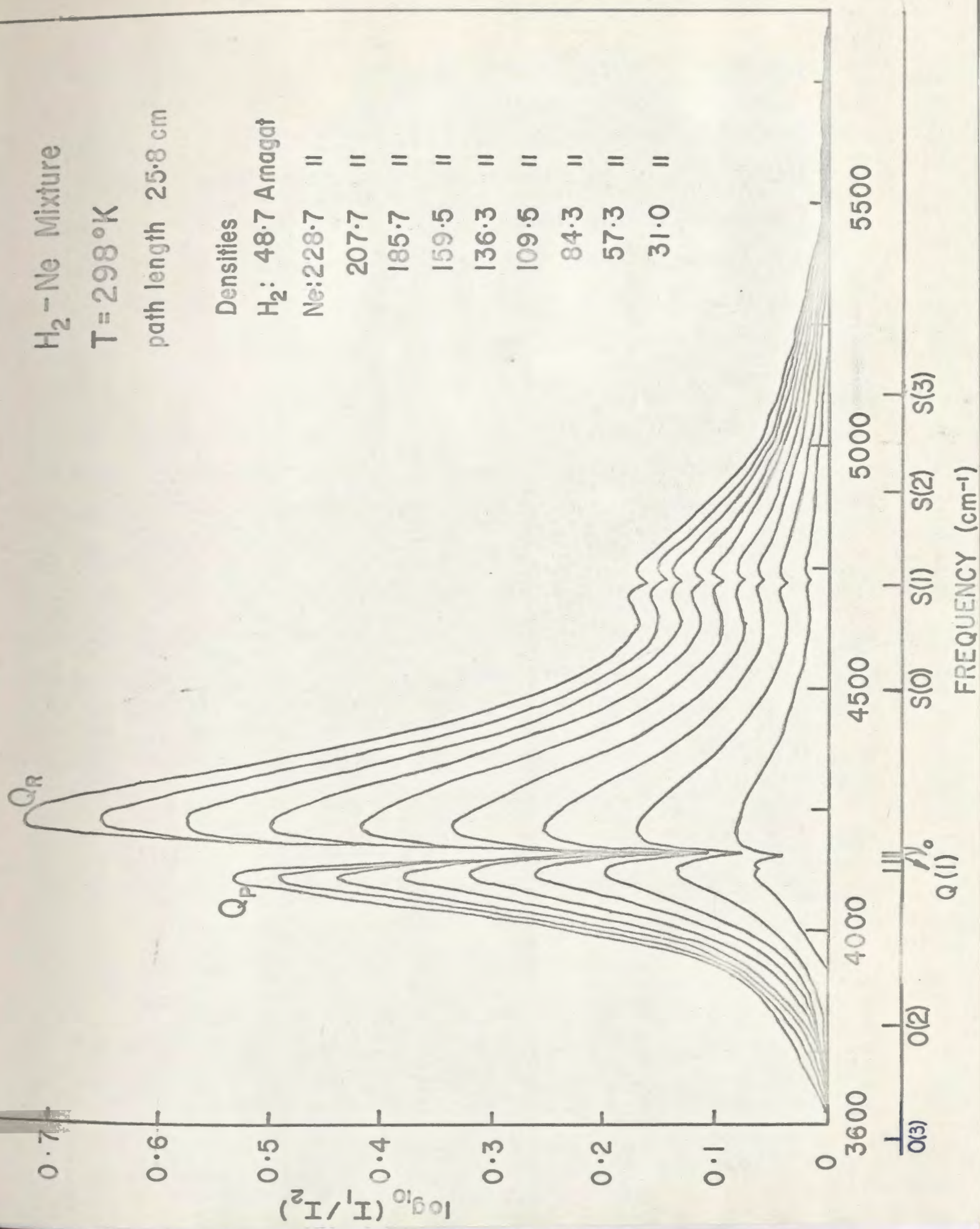
directly from the isothermal data for Ne (Michels, Wassenaar, and Louwerse, 1960) and for Kr (Trappeniers, Wassenaar, and Wolkers, 1966). Here  $(\rho_a)_P$  and  $(\rho_b)_P$  are the densities of hydrogen and the foreign gas respectively, at a pressure,  $P$ , equal to the total pressure of the mixture, which were also obtained directly from the isothermal data. This approximate interpolation method of obtaining the partial density of a foreign gas in a binary mixture was used by Cho et al (1963), and Reddy et al (1965) and it was shown that this method is accurate enough within experimental error.

CHAPTER 3

EXPERIMENTAL RESULTS

3.1 Absorption Profiles: Two typical sets of experimental profiles of the enhancement of absorption of the induced fundamental band of hydrogen - one obtained in H<sub>2</sub>-Ne mixtures with a base density, 48.7 Amagat of hydrogen, and the other in H<sub>2</sub>-Kr mixtures with a base density, 14.2 Amagat of hydrogen, are presented in Figs. 5, and 6, respectively. The positions of the band origin,  $\nu_0$ , and the individual lines of the O, Q, and S branches were calculated from the known molecular constants of hydrogen (Stoicheff, 1957) and were marked on the frequency axis. The calculation of frequencies was made under the assumption that the frequency structure of the band was the same as that of the Raman Spectrum of the low pressure gas. This assumption is justified since no perturbation of the molecular constants in the induced absorption spectrum of the hydrogen gas was observed. Just as in the contours of the fundamental band of hydrogen in pure H<sub>2</sub> and in H<sub>2</sub>-He, H<sub>2</sub>-A, and H<sub>2</sub>-N<sub>2</sub> mixtures obtained by earlier investigators, the important characteristic of the profiles obtained in the present investigation in H<sub>2</sub>-Ne and H<sub>2</sub>-Kr mixtures is the splitting of the Q branch into two well-resolved components Q<sub>P</sub> and Q<sub>R</sub> as shown in Figs. 5 and 6. The minima between these components occur at the position of Q(1) (4155 cm<sup>-1</sup>) instead of at the band origin,  $\nu_0$  ( Q (0): 4161 cm<sup>-1</sup> ). The components Q<sub>R</sub> and Q<sub>P</sub> have been interpreted (Chisholm et al, 1954; Hare et al, 1958) as due to the summation and difference tones  $\nu_0 \pm \nu_k$  where  $\nu_0$  (in cm<sup>-1</sup>) is

Fig. 5 The enhancement of absorption of the fundamental band of hydrogen in hydrogen-neon mixtures.



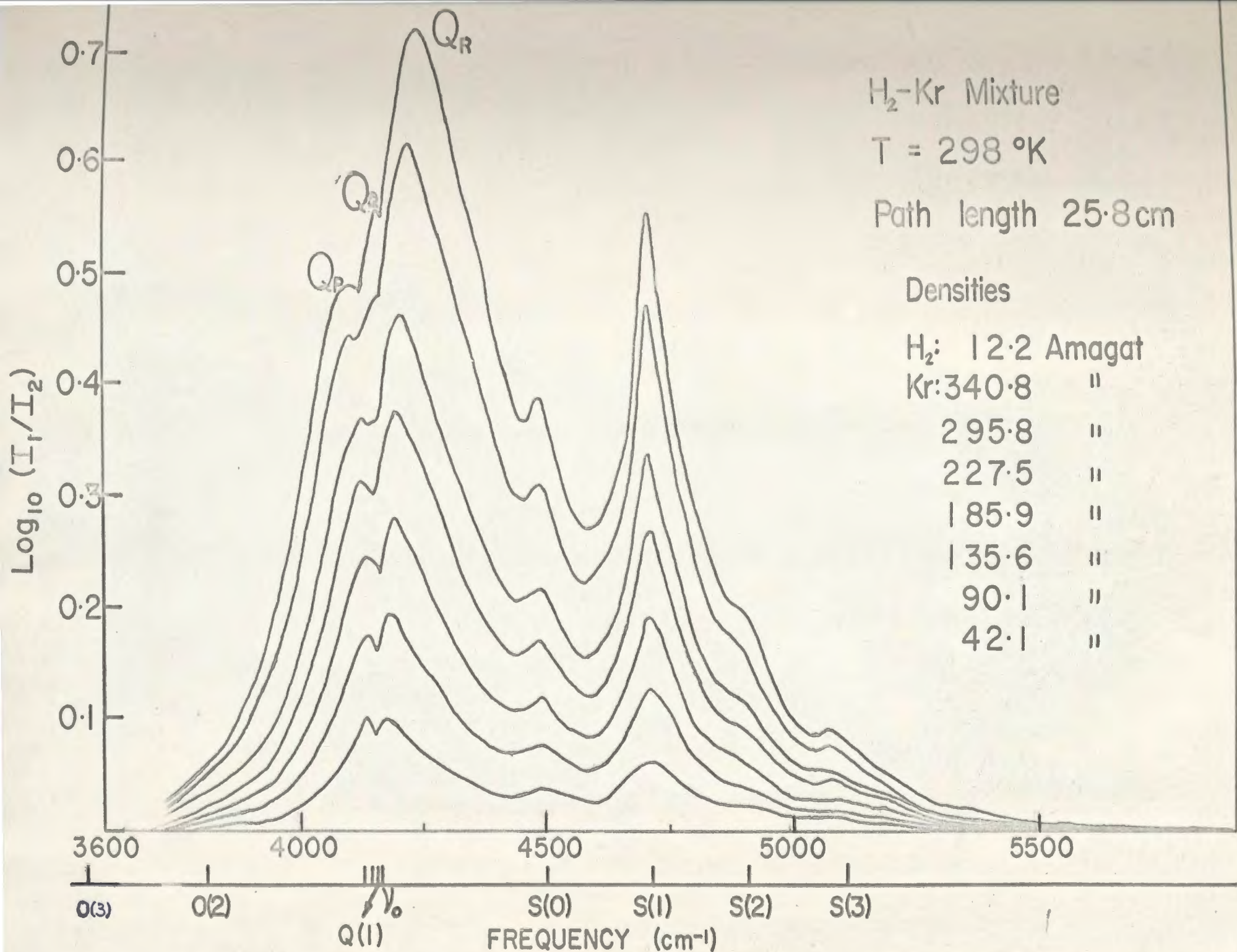


Fig. 6 The enhancement of absorption of the fundamental band of hydrogen in hydrogen-krypton mixtures.

the frequency of the molecular vibration which corresponds to the vibrational transition in hydrogen,  $v' = 1 \leftarrow v'' = 0$ , and  $\nu_k$  (in  $\text{cm}^{-1}$ ) is the continuum of translational (kinetic) frequencies that are exchanged by the absorbing hydrogen molecules and the perturbing molecules during collisions. The high frequency component,  $Q_R$ , results if the absorbing photon, in addition to changing the vibrational energy of the hydrogen molecule, increases the relative kinetic energy of the colliding molecules. On the other hand, the low frequency component,  $Q_P$ , results when the relative kinetic energy of the colliding system contributes to a photon which would otherwise have inadequate energy to cause the vibrational transition.

An interesting feature of the contours obtained in  $\text{H}_2$ -Ne mixtures is that the  $Q_P$  component at low densities and the  $S(1)$  component at all densities show doublet structures. This type of doublet structures in the fundamental band of hydrogen in pure  $\text{H}_2$  and in  $\text{H}_2$ -A mixtures under various conditions of temperature and pressure has been studied and discussed by Gush et al (1957). The  $Q_P$  doublet structure observed at low pressures can be understood by the consideration that each one of the components of the Q branch,  $Q(0)$ ,  $Q(1)$ ,  $Q(2)$ ,  $Q(3)$ , ---- has a profile similar to a Bjerrum double band. The disappearance of the same, when the density of the foreign gas is increased, is due to the fact that at higher densities, the main maxima  $Q_P$  and  $Q_R$  become more diffuse and their separation becomes larger. The striking splitting of the  $S(1)$  line reveals that there is a considerable amount of contribution of the electron overlap interaction to the  $S(1)$  line which has been considered so far

to arise almost completely due to quadrupolar interaction.

Within the range of densities used in the present investigation the shapes of the contours for different mixtures with a given perturbing gas remain the same except that the separation of the  $Q_p$  and  $Q_R$  maxima,  $\Delta \nu_{PR}^{\max}$ , increases with the increasing density of the mixture.  $\Delta \nu_{PR}^{\max}$  varies from  $75 \text{ cm}^{-1}$  to  $90 \text{ cm}^{-1}$  for the contours obtained with  $\text{H}_2$ -Ne mixtures, and from  $40 \text{ cm}^{-1}$  to  $70 \text{ cm}^{-1}$  for the contours with  $\text{H}_2$ -Kr mixtures, presented in Figs. 5 and 6 respectively.

No splitting of the  $Q_p$  and  $S(1)$  lines has been observed in the  $\text{H}_2$ -Kr mixtures at the densities used in the present investigation. But there is an indication of the  $Q_Q$  component in the Q branch at higher densities (Fig.6). The quadrupolar components  $0(2)$ ,  $Q_Q$ ,  $S(0)$ ,  $S(1)$ ,  $S(2)$ , and  $S(3)$  obtained in  $\text{H}_2$ -Kr mixtures are much more pronounced than those obtained in  $\text{H}_2$ -Ne mixtures. This was not unexpected since the polarizability of krypton ( $\alpha_{\text{Kr}} = 16.8 \text{ a}_0^3$ ) is much larger than that of neon ( $\alpha_{\text{Ne}} = 2.7 \text{ a}_0^3$ ).

In order to compare the overall absorption arising from the binary collisions of the molecules, the experimental profiles of the enhancement of absorption of  $\text{H}_2$ -Ne and  $\text{H}_2$ -Kr mixtures along with that of the pure hydrogen experiment, which was obtained for the purpose of checking the reliability of the apparatus, were plotted in Fig. 7. Here the contours chosen were approximately of the same density product  $\rho_a \rho_b$ , where "a" and "b" refer to the absorbing hydrogen gas and the perturbing gas respectively, and  $\rho_b \equiv \rho_a$  for the pure hydrogen experiment.

A detailed analysis of the profiles of the fundamental

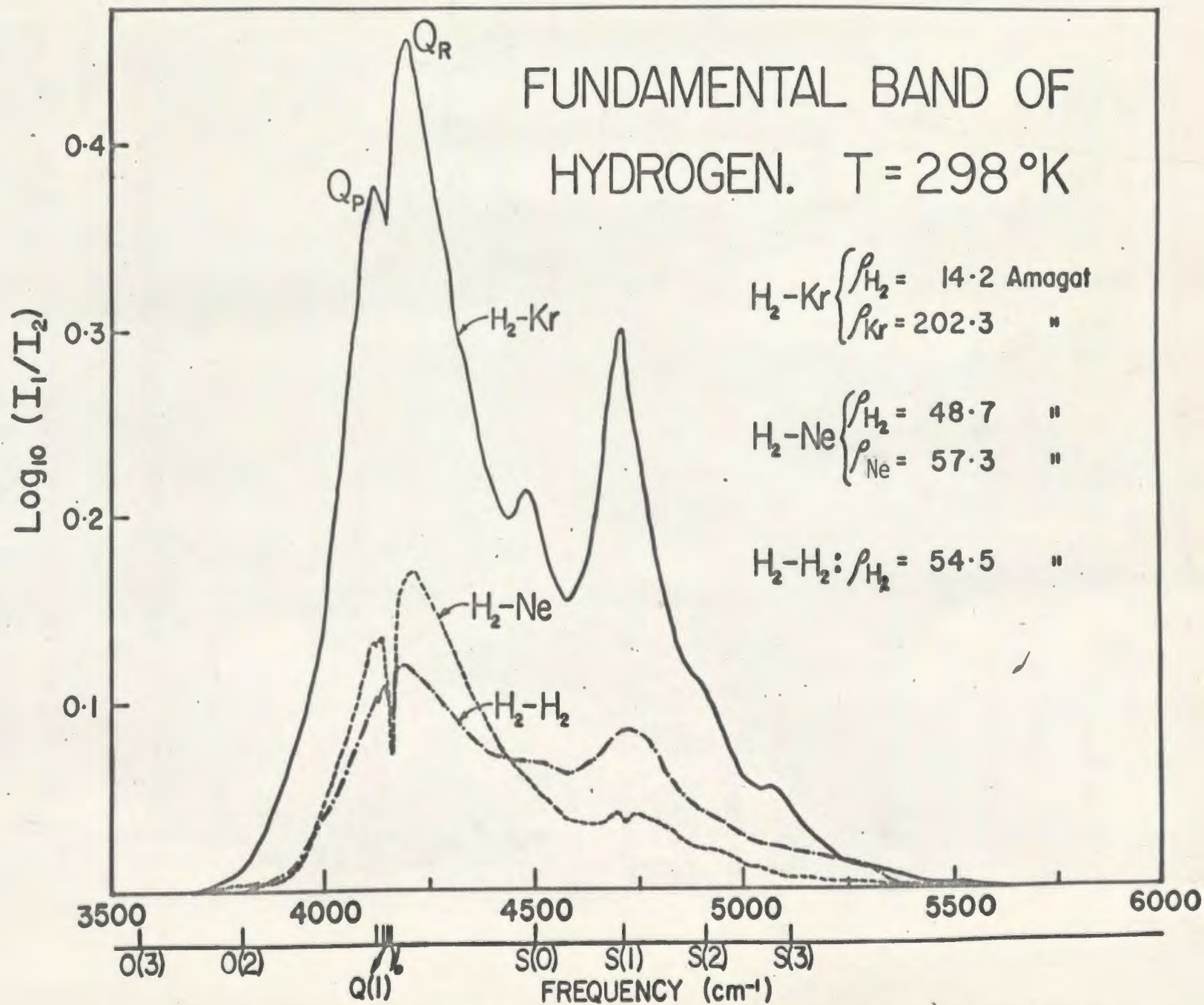


Fig. 7 Comparison of the enhancements of absorption of the fundamental band of hydrogen in  $H_2\text{-H}_2$ ,  $H_2\text{-Ne}$  and  $H_2\text{-Kr}$  mixtures.

infrared band of hydrogen in H<sub>2</sub>-Ne and H<sub>2</sub>-Kr mixtures will be presented in chapter 5 of this thesis.

### 3.2 Absorption Coefficients

By calculating the area under the experimental contours, the integrated absorption coefficients of the enhancement per unit path length,  $\int \alpha_{en}(\nu) d\nu$  in cm<sup>-1</sup>/cm, have been obtained and correlated with the mixture densities in Table I and II respectively for H<sub>2</sub>-Ne and H<sub>2</sub>-Kr mixture experiments. The dependence of the integrated absorption coefficient on the density of the perturbing gas,  $\rho_b$ , has been obtained by plotting  $\frac{1}{\rho_a \rho_b} \int \alpha_{en}(\nu) d\nu$  against  $\rho_b$  for both H<sub>2</sub>-Ne and H<sub>2</sub>-Kr mixture experiments as shown in Fig. 8. The straight line relations indicate that the integrated absorption coefficients can be represented in the form,

$$\int \alpha_{en}(\nu) d\nu = \alpha_{1b} \rho_a \rho_b + \alpha_{2b} \rho_a \rho_b^2 \quad (3-1)$$

where  $\alpha_{1b}$  and  $\alpha_{2b}$  are the binary and ternary absorption coefficients of the enhancement respectively. The values of these coefficients have been obtained by means of least squares fit and are summarized in Table III. In Table V, the modified binary absorption coefficients  $\tilde{\alpha}_{1b}$  are also included. The binary and ternary absorption coefficients of the band at room temperature in H<sub>2</sub>-H<sub>2</sub>, H<sub>2</sub>-He, H<sub>2</sub>-A, and H<sub>2</sub>-N<sub>2</sub> obtained earlier by Hare and Welsh (1958) are also included in Table III. The modified binary and ternary absorption coefficients,  $\tilde{\alpha}_{1b}$  and  $\tilde{\alpha}_{2b}$  are related to the integrated absorption coefficients by the equation

$$c \int \tilde{\alpha}_{en}(\nu) d\nu = \tilde{\alpha}_{1b} \tilde{\rho}_a \tilde{\rho}_b + \tilde{\alpha}_{2b} \tilde{\rho}_a \tilde{\rho}_b^2 \quad (3-2)$$

Fig. 8 The relation between the enhancements in the integrated absorption coefficients of the fundamental band of hydrogen and the partial densities  $\rho_a$  and  $\rho_b$  in  $H_2$ -Ne and  $H_2$ -Kr mixtures at room temperature.

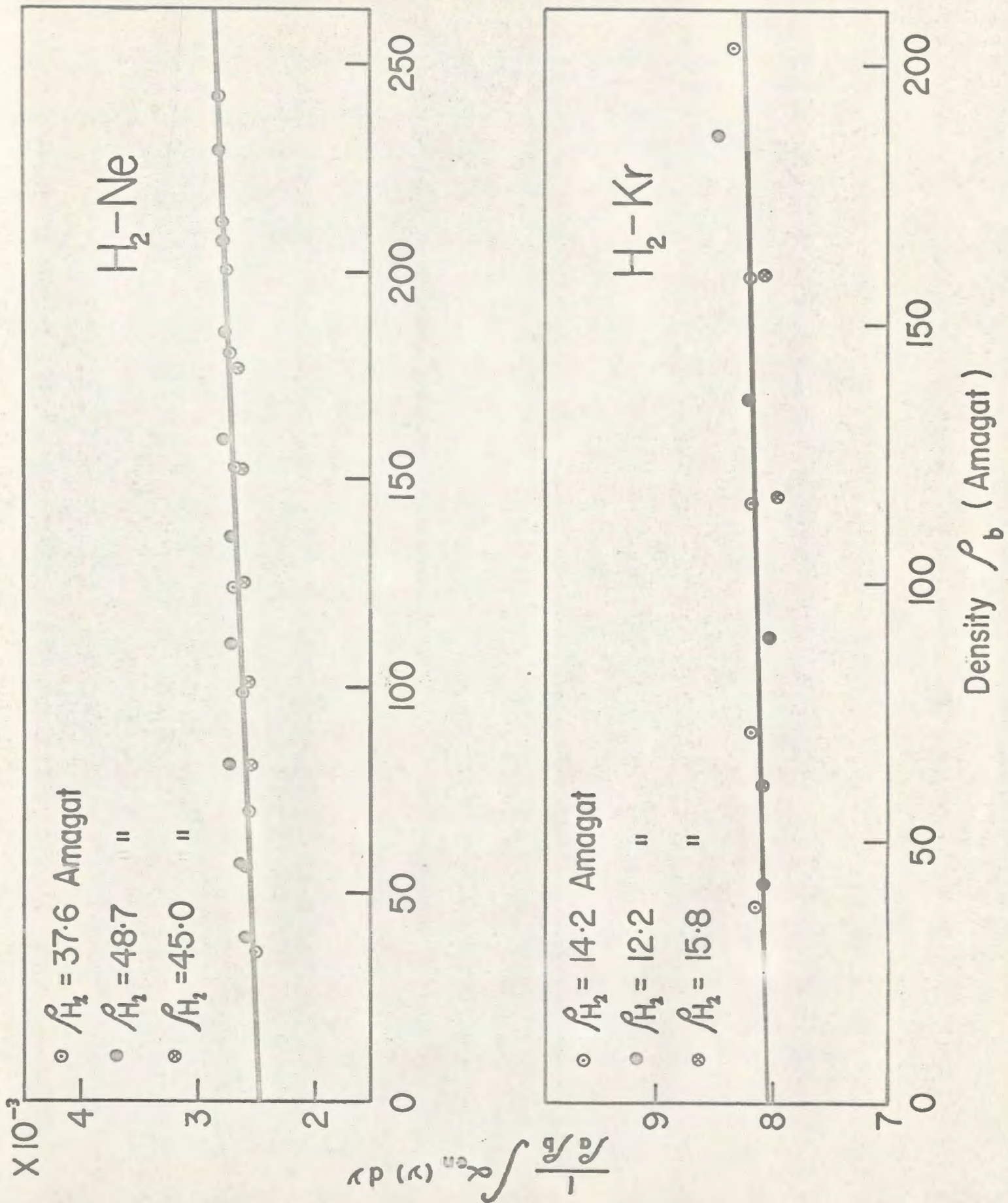


TABLE I

Enhancement of the Integrated Absorption Coefficient of the H<sub>2</sub> Fundamental Band in H<sub>2</sub>-Ne Mixtures  
at Room Temperature

$\rho_{\text{H}_2}$ (Amagat)	$\rho_{\text{Ne}}$ (Amagat)	$\int \alpha_{\text{en}}(\nu) d\nu$ (cm <sup>-1</sup> /cm)	$\rho_{\text{H}_2}$ (Amagat)	$\rho_{\text{Ne}}$ (Amagat)	$\int \alpha_{\text{en}}(\nu) d\nu$ (cm <sup>-1</sup> /cm)
37.6	36.6	3.46	45.0	101.5	11.72
"	69.2	6.67	"	126.5	14.69
"	98.8	9.78	"	152.0	17.59
"	123.4	12.60	"	177.0	20.88
"	152.5	15.54	48.7	31.0	3.16
"	180.5	18.60	"	57.3	6.91
"	199.8	20.86	"	84.3	11.14
"	224.1	23.75	"	109.5	14.58
"	242.9	25.76	"	136.3	18.08
45.0	32.3	3.37	"	159.5	21.63
"	57.0	6.49	"	185.7	24.97
"	81.4	9.22	"	207.7	28.06
-	-	-	"	228.7	31.37

Table II

Enhancement of the Integrated Absorption Coefficient of the H<sub>2</sub> Fundamental Band in H<sub>2</sub>-Kr Mixtures at Room Temperature.

$\rho_{\text{H}_2}$ (Amagat)	$\rho_{\text{Kr}}$ (Amagat)	$\int \alpha_{\text{en}}(\nu) d\nu$ (cm <sup>-1</sup> /cm)
12.2	42.1	4.33
12.2	90.1	8.75
12.2	135.6	13.73
12.2	185.9	19.31
14.2	37.7	4.35
14.2	71.3	8.26
14.2	116.0	13.42
14.2	159.0	18.43
14.2	202.3	23.79
15.8	61.1	7.79
15.8	116.3	14.57
15.8	159.4	20.09
15.8	217.0	29.09

Table III

Absorption coefficients of the induced fundamental band of hydrogen at room temperature.

Mixture	Binary Absorption coefficient ( $10^{-3}\text{cm}^{-2}\text{ Amagat}^{-2}$ )	Ternary absorption coefficient ( $10^{-6}\text{ cm}^{-2}\text{ Amagat}^{-3}$ )
<u>Present work:</u>		
H <sub>2</sub> - Ne	$\alpha_{1b}: 2.50 \pm 0.01$	$\alpha_{2b}: 1.3$
H <sub>2</sub> - Kr	$8.02 \pm 0.01$	0.9
<u>Earlier Work:*</u>		
H <sub>2</sub> - H <sub>2</sub>	$\alpha_{1a}: 2.4$	$\alpha_{2a}: 3.9$
H <sub>2</sub> - He	$\alpha_{1b}: 1.1$	$\alpha_{2b}: 0.55$
H <sub>2</sub> - A	4.1	3.9
H <sub>2</sub> - N <sub>2</sub>	5.4	5.5

\*Hare, W.F.J. and Welsh, H.L. 1958. Can. J. Phys. 36, 88.

where  $\tilde{\alpha}_{en}(\nu) = \alpha_{en}(\nu)/\nu$  is the absorption coefficient of enhancement at frequency  $\nu$  with the frequency factor removed,  $\tilde{\rho}_a$  and  $\tilde{\rho}_b$  are the partial number densities of the absorbing gas and the perturbing gas respectively and  $c$  is the speed of light. These new quantities are related to the quantities in eq. (3-1) by the following equations:

$$\tilde{\alpha}_{1b} = \frac{c\alpha_{1b}}{\bar{\nu}} \left( \frac{V_0}{N_A} \right)^2 \quad (3-3)$$

$$\tilde{\alpha}_{2b} = \frac{c\alpha_{2b}}{\bar{\nu}} \left( \frac{V_0}{N_A} \right)^3 \quad (3-4)$$

$$\tilde{\rho}_a = \rho_a \frac{N_A}{V_0} \quad (3-5)$$

$$\tilde{\rho}_b = \rho_b \frac{N_A}{V_0} \quad (3-6)$$

where  $V_0$  is the gram-molecular volume of the gas at N.T.P.,  $N_A$  is Avogadro's number, and  $\bar{\nu}$ , which is defined by

$$\bar{\nu} = \int \nu \alpha_{en}(\nu) d\nu / \int \nu^{-1} \alpha_{en}(\nu) d\nu \quad (3-7)$$

is the center of the band which is  $4338 \text{ cm}^{-1}$  for  $\text{H}_2$ -Ne mixtures and  $4388 \text{ cm}^{-1}$  for  $\text{H}_2$ -Kr mixtures, and they are found to be approximately the same for various densities of the same experiment.

The physical picture of the binary and ternary absorption coefficients  $\alpha_{1b}$  and  $\alpha_{2b}$  is that  $\alpha_{1b}$  arises from the binary collisions of the hydrogen molecules with the foreign gas molecules and  $\alpha_{2b}$  arises from the ternary collisions of the type with one hydrogen molecule and two foreign gas molecules. The modified binary absorption coefficient  $\tilde{\alpha}_{1b}$  (in  $\text{cm}^6 \text{ sec}^{-1}$ ) actually stands for the

transition probability of absorption because it does not depend on the frequency factor.

The ternary term  $\alpha_{2b}\rho_a\rho_b^2$  in equation (3-1) has been interpreted by previous authors (Hare and Welsh, 1958) as being the combination of the following three factors: i) the finite volume effect, ii) ternary collisions, and iii) the change of molecular polarizability with pressure. The effect of finite volume was described by Chisholm and Welsh (1954). At low densities the number of absorption-inducing collisions is proportional to  $\rho_a\rho_b$ . However, when the volume of the molecules themselves becomes an appreciable fraction of the space which they occupy, the number of collisions increases more rapidly than the product  $\rho_a\rho_b$ . Secondly, when a molecule is surrounded by a symmetrical configuration of perturbing molecules, the induced transition moment of the molecule is zero. Hence, ternary and higher order collisions would annul to some extent the action of binary collisions. This has been referred to as a "cancellation effect". Thirdly, a decrease in atomic and molecular polarizabilities at high densities was predicted by quantum mechanical considerations (Michels, de Boer, and Bijl 1937; de Groot and ten Seldam 1947). This would lower the integrated absorption coefficient to some extent but the magnitude of the effect is difficult to estimate.

It may be noted that another possible ternary term  $\alpha_{2ab}\rho_a^2\rho_b$  due to collisions between two hydrogen molecules and one foreign gas molecule is missing in equation (3-1). This is believed to be mainly due to the limited experimental accuracy in the deduction of the experimental results and the smallness of the ternary coefficient  $\alpha_{2ab}$ .

CHAPTER 4

THEORY AND CALCULATIONS

After the discovery of the pressure induced infrared absorption spectra of homonuclear diatomic molecules at the University of Toronto in 1949, the theory of the fundamental bands of these molecules in compressed pure gases and their binary mixtures with foreign gases was given by Van Kranendonk and Bird (1951a, 1951b), Van Kranendonk (1952, 1957, 1958, 1959), and Britton and Crawford (1958).

4.1 Theory

According to the so-called "exp-4" model proposed by Van Kranendonk (1958), the absorption arises due to the dipole moment induced by intermolecular forces in the course of collisions in the molecular cluster. The dipole moment induced in a collision between a homonuclear diatomic molecule and a perturbing molecule consists of two additive parts: i) a short-range angle-independent overlap moment and ii) a long-range angle-dependent moment. The short-range moment, of strength  $\xi$  and range  $\rho$  occurs as a result of distortion of the electronic configuration of molecules in a collision due to short-range overlap forces and decreases exponentially with increasing intermolecular distance  $R$ . The other moment results from the polarization of one molecule by the quadrupole field of the other and is proportional to  $R^{-4}$ . It depends on the derivatives of the quadrupole moment and the average polarizability of the absorbing molecule at the equilibrium position,  $Q_1' (= (\frac{\partial Q_1}{\partial r_1})_0)$  and  $\alpha_1' (= (\frac{\partial \alpha_1}{\partial r_1})_0)$  respectively and the quadrupole moment and the average polarizability

of the perturbing molecule,  $Q_2$  and  $\alpha_2$  respectively. Here  $r_1$  is the internuclear distance of the absorbing molecule.

The induced dipole moment  $M$  of a pair consisting of a homonuclear diatomic molecule and a perturbing molecule, can be represented as (Van Kranendonk 1958)

$$M(\omega_1, \omega_2, R_{12}) = 4\pi \sum_{\lambda_1 \mu_1, \lambda_2 \mu_2} D(\lambda_1 \mu_1, \lambda_2 \mu_2; R_{12}) Y_{\lambda_1}^{\mu_1}(\omega_1) Y_{\lambda_2}^{\mu_2}(\omega_2) \quad (4-1)$$

where  $\omega_1 = (\theta_1, \phi_1)$  and  $\omega_2 = (\theta_2, \phi_2)$  specify the polar angles of the internuclear axes of the molecules 1 and 2, relative to a co-ordinate frame  $xyz$ , the  $z$  axis of which lies along the vector  $R_{12}$  that connects the center of mass of molecule 1 to that of molecule 2; and  $\mu_1$  and  $\mu_2$  are the projection quantum numbers of the angular momenta  $\lambda_1$  and  $\lambda_2$  along an axis perpendicular to  $R_{12}$ . The components  $D_\mu$  of the expansion coefficient  $D$  in the same co-ordinate frame are characteristic of the pair of colliding molecules.  $\mu$  takes values 1, 0, and -1 and

$$D_{\pm 1} = 2^{-\frac{1}{2}} (D_x \pm iD_y) ; \quad D_0 = D_z \quad (4-2)$$

For homonuclear diatomic molecules, the "exp-4" model for the induced moment implies that the components  $D_\mu$  are assumed to have the following values:

$$D_0(00,00) = \xi \exp(-R/\rho) \quad (4-3)$$

$$D_0(20,00) = \frac{3}{\sqrt{5}} \frac{Q_1 \alpha_2}{R^4} \quad (4-4)$$

$$D_0(00,20) = -\frac{3}{\sqrt{5}} \frac{\alpha_1 Q_2}{R^4} \quad (4-5)$$

$$D_{\pm 1}(2\pm 1; 00) = + \frac{3}{\sqrt{15}} \frac{Q_1^i \alpha_2}{R^4} \quad (4-6)$$

$$D_{\pm 1}(00; 2\pm 1) = - \frac{3}{\sqrt{15}} \frac{\alpha_1 Q_2^i}{R^4} \quad (4-7)$$

The functions  $Y_{\lambda}^{\mu}(\omega)$  in equation (4-1) are spherical harmonics which can be expressed as:

$$Y_{\lambda}^{\mu}(\omega) = ( (2\lambda+1)(\lambda-\mu)! / 4\pi(\lambda+\mu)! )^{\frac{1}{2}} \rho_{\lambda}^{\mu}(\cos\theta) e^{i\mu\phi} \quad (4-8)$$

and are dimensionless. Therefore, the seven non-vanishing coefficients  $D(\lambda_1\mu_1, \lambda_2\mu_2)$  have the dimensions of dipole moment. If molecules 1 and 2 are identical there is a center of symmetry at the midpoint of  $R_{12}$ . The first coefficient  $D_0(00; 00)$  which decreases exponentially with the increasing intermolecular distance  $R$  can be considered as the dipole moment that is induced by the short-range overlap forces, while the other four coefficients in equations (4-4) to (4-7) can be thought of as the contributions of the long-range forces to the induced dipole moment.

The integrated induced absorption coefficient  $\int \alpha(\nu) d\nu$ , where the absorption coefficient,  $\alpha(\nu)$ , at frequency  $\nu$ , is defined by Beer's law,

$$I = I_0 \exp(-\alpha(\nu)l) \quad (4-9)$$

can be generally expressed in terms of the powers of the density of the gas. For the pure gas, at a density  $\rho_a$ , it has the form

$$\int \alpha(\nu) d\nu = \alpha_{1a} \rho_a^2 + \alpha_{2a} \rho_a^3 + \dots \quad (4-10)$$

For a binary gas mixture, the enhancement of absorption due to the addition of a foreign gas with a particular density  $\rho_b$  to the pure

gas at a density  $\rho_a$  is given by

$$\int \alpha_{en}(\nu) d\nu = \alpha_{1b} \rho_a \rho_b + \alpha_{2b} \rho_a \rho_b^2 + \dots \quad (4-11)$$

Here  $\alpha_{1a}$  or  $\alpha_{1b}$  ( $\text{cm}^{-2} \text{Amagat}^{-2}$ ) is the binary coefficient and  $\alpha_{2a}$  or  $\alpha_{2b}$  ( $\text{cm}^{-2} \text{Amagat}^{-3}$ ) is the ternary absorption coefficient and the densities  $\rho_a$  and  $\rho_b$  are expressed in Amagat unit. In order to make the absorption coefficients more directly connected to the transition probability rather than to the observed intensity, the absorption coefficients  $\alpha_{1a}$  and  $\alpha_{1b}$  are converted into a new form by the following equations:

$$\bar{\alpha}_{1a} = \frac{c\alpha_{1a}}{\bar{\nu}} (V_0/N_A)^2 \quad ; \quad \bar{\alpha}_{2a} = \frac{c\alpha_{2a}}{\bar{\nu}} (V_0/N_A)^3 \quad (4-12)$$

$$\bar{\alpha}_{1b} = \frac{c\alpha_{1b}}{\bar{\nu}} (V_0/N_A)^2 \quad ; \quad \bar{\alpha}_{2b} = \frac{c\alpha_{2b}}{\bar{\nu}} (V_0/N_A)^3 \quad (4-13)$$

Here

$$\bar{\nu} = \int \alpha(\nu) d\nu / \int \alpha(\nu) \nu^{-1} d\nu \quad (4-14)$$

is the center of the band,  $V_0$  is the gram molecular volume at N.T.P.,  $N_A$  is the Avogadro number,  $c$  is the speed of light and  $\nu$  is the frequency expressed in wave numbers,  $\text{cm}^{-1}$ . The integrated absorption coefficients (4-10) and (4-11) are then expressed as follows:

$$c \int \bar{\alpha}(\nu) d\nu = \bar{\alpha}_{1a} \bar{\rho}_a^2 + \bar{\alpha}_{2a} \bar{\rho}_a^3 + \dots \quad (4-15)$$

$$c \int \bar{\alpha}_{en}(\nu) d\nu = \bar{\alpha}_{1b} \bar{\rho}_a \bar{\rho}_b + \bar{\alpha}_{2b} \bar{\rho}_a \bar{\rho}_b^2 + \dots \quad (4-16)$$

where  $\bar{\alpha}(\nu) = \alpha(\nu)/\nu$  is an absorption coefficient independent of frequency, and  $\bar{\rho}_a$  and  $\bar{\rho}_b$  are number densities of the absorbing gas "a" and the perturbing gas "b" respectively in a given mixture.

According to Van Kranendonk (1957), the binary absorption coefficient of a definite rotational branch B of the fundamental

vibrational band of a pure homonuclear diatomic gas is given by

$$\tilde{\alpha}_{1a}(B) = \kappa \sum^{(B)} P_1 P_2 \int |M(\omega_1 \omega_2 R_{12})|^2 g_0(R_{12}) dR_{12} \quad (4-17)$$

where  $\kappa = \frac{\pi}{3m_0 v_0}$ ,  $m_0$  being the reduced mass of the absorbing molecule

and,  $v_0$  being the frequency of molecular oscillation (in  $\text{sec}^{-1}$ ),

$P_i$  is the normalized Boltzmann factor for molecule  $i$ , which is normalized in such a way that

$$\sum_{J=0}^{\infty} P_i(J)(2J+1) = 1 \quad (4-18)$$

$$J = 0$$

and  $g_0(R_{12})$  is the pair distribution function arising from the pair of molecules (1,2). The selection rule for the rotational quantum number  $J$ , is  $\Delta J = 0, \pm 2$ , i.e. the band consists of the Q, S, and O branches. The binary absorption coefficients for individual lines of the O, Q, and S branches of the induced fundamental band are expressed as follows: For the pure gas

$$\tilde{\alpha}_{1a}(O(J)) = (\mu_1^2 + \mu_2^2) \mathbf{J} \tilde{\gamma} P(J) L_2(J, J-2), \quad (4-19)$$

$$\begin{aligned} \tilde{\alpha}_{1a}(Q(J)) = & \lambda^2 \mathbf{I} \tilde{\gamma} P(J) L_0(J, J) + \mu_1^2 \mathbf{J} \tilde{\gamma} P(J) L_2(J, J) \\ & + \mu_2^2 \mathbf{J} \tilde{\gamma} P(J) L_0(J, J) \sum_{J'} P(J') L_2(J', J'), \end{aligned} \quad (4-20)$$

and

$$\tilde{\alpha}_{1a}(S(J)) = (\mu_1^2 + \mu_2^2) \mathbf{J} \tilde{\gamma} P(J) L_2(J, J+2). \quad (4-21)$$

For the mixtures

$$\tilde{\alpha}_{1b}(O(J)) = (\mu_1^2 + \mu_2^2) \mathbf{J} \tilde{\gamma} P(J) L_2(J, J-2), \quad (4-22)$$

$$\begin{aligned} \tilde{\alpha}_{1b}(Q(J)) = & \lambda^2 \mathbf{I} \tilde{\gamma} P(J) L_0(J, J) + \mu_1^2 \mathbf{J} \tilde{\gamma} P(J) L_2(J, J) \\ & + \mu_2^2 \mathbf{J} \tilde{\gamma} P(J) L_0(J, J), \end{aligned} \quad (4-23)$$

and

$$\tilde{\alpha}_{1b}(S(J)) = (\mu_1^2 + \mu_2^2) \mathbf{J} \tilde{\gamma} P(J) L_2(J, J+2). \quad (4-24)$$

The dimensionless parameters  $\mu_1$ ,  $\mu_2$ , and  $\lambda$  are defined as

$$\mu_1 = \frac{Q_1' \alpha_2}{e \sigma^4} \quad (4-25)$$

$$\mu_2 = \frac{\alpha_1' Q_2}{e \sigma^4} \quad (4-26)$$

$$\lambda = \frac{\xi}{e} \exp(-\sigma/\rho) \quad (4-27)$$

where  $\sigma$  is the intermolecular distance  $R$  for which the intermolecular potential is zero and  $e$  is the absolute value of the electronic charge.

$\tilde{\gamma}$  is defined by

$$\tilde{\gamma} = \frac{\pi e^2 \sigma^3}{3m_0 v_0} \quad (4-28)$$

which has the dimension of an integrated absorption coefficient per (density)<sup>2</sup>. The radial distribution integrals  $\mathbf{I}$  and  $\mathbf{J}$  are defined as

$$\mathbf{I} = 4\pi \int_0^\infty \exp(-2(x-1)\sigma/\rho) g_0(x) x^2 dx \quad (4-29)$$

$$\mathbf{J} = 12\pi \int_0^\infty x^{-8} g_0(x) x^2 dx \quad (4-30)$$

where  $x = R/\sigma$  and  $g_0(x)$  is the low density limit of the pair distribution function. The dimensionless quantities  $L_\lambda(J, J')$  are Racah coefficients, whose non-vanishing values for  $\lambda = 0$  and  $2$  are given by

$$\begin{aligned} L_0(J, J) &= (2J+1) \\ L_2(J, J-2) &= 3(J-1)J/2(2J-1) \\ L_2(J, J) &= J(J+1)(2J+1)/(2J-1)(2J+3) \\ L_2(J, J+2) &= 3(J+1)(J+2)/2(2J+3) \end{aligned} \quad (4-31)$$

The normalized Boltzman factors  $P(J)$  for hydrogen in various rotational states of the ground vibrational level, occurring in equations (4-19) to (4-24) is given by

$$P(J) = \frac{g_n \exp(-J(J+1)B_0 hc/kT)}{\sum_J (2J+1) g_n \exp(-J(J+1)B_0 hc/kT)} \quad (4-32)$$

where  $g_n = (2T+1)$  is the nuclear spin degeneracy,  $T$  being the total nuclear spin of the molecule. When the perturbing molecules,  $b$ , are monatomic,  $\mu_2 = 0$ , because  $Q_2$  equals zero.

By using the property of Racah coefficients,

$$\sum_{J', \lambda} L(J, J') = (2J+1), \quad (4-33)$$

the total binary absorption coefficients  $\bar{\alpha}_{1a}$  and  $\bar{\alpha}_{1b}$  for the fundamental band are obtained by adding, after summation over  $J$ , the binary absorption coefficients  $\bar{\alpha}_{1a}(O(J))$ ,  $\bar{\alpha}_{1a}(Q(J))$ , and  $\bar{\alpha}_{1a}(S(J))$  for the pure gas and  $\bar{\alpha}_{1b}(O(J))$ ,  $\bar{\alpha}_{1b}(Q(J))$ , and  $\bar{\alpha}_{1b}(S(J))$  for a binary mixture respectively. The resulting single expression for both cases can be written as

$$\bar{\alpha}_{1a} \text{ or } \bar{\alpha}_{1b} = \lambda^2 \mathbf{I} \tilde{\gamma} + (\mu_1^2 + \mu_2^2) \mathbf{J} \tilde{\gamma} \quad (4-34)$$

where the first term  $\lambda^2 \mathbf{I} \tilde{\gamma}$  is the overlap part and the second term  $(\mu_1^2 + \mu_2^2) \mathbf{J} \tilde{\gamma}$  is the quadrupole part.

The above theory of Van Kranendonk for pressure induced absorption almost runs parallel to the theory of the equation of state of gases. The density expansion of the integrated absorption coefficient (egs. 4-15 and 4-16) is similar to the virial expansion of the pressure where the second and third virial coefficients are the counterparts of the binary and ternary absorption coefficients.

The absorption coefficients provide information about induced deformation of the electronic configuration of the molecules, while the virial coefficients give information about the intermolecular forces.

#### 4.2 Calculations

In the theoretical expression (4-34) for the binary absorption coefficient, it is possible to calculate the quadrupole part  $(\mu_1^2 + \mu_2^2) \mathbf{J} \bar{\gamma}$  and the factor  $\mathbf{I} \bar{\gamma}$  in the overlap parameter,  $\lambda^2 \mathbf{I} \bar{\gamma}$ . Then, by fitting the theoretical expression (4-34) to the experimental values obtained by us in the present investigation and earlier by Hare and Welsh (1958), the values of  $\lambda$  for different mixtures can be obtained. In the following paragraphs, details of these calculations are described; a relation connecting the values of  $\lambda$  with the corresponding values of the parameter,  $\epsilon$ , of the Lennard-Jones potentials for the mixtures is proposed; and the binary absorption coefficients of the individual lines of the O, Q, and S branches are calculated.

The classical values ( $\mathbf{I}_{cl}$  and  $\mathbf{J}_{cl}$ ) of the radial distribution integrals  $\mathbf{I}$  and  $\mathbf{J}$  given by eqs. (4-29) and (4-30) can be calculated, for high temperatures, using the classical pair distribution function

$$g_0(x) = \exp(-V(x)/kT) \quad (4-35)$$

where  $V(x)$  is the Lennard-Jones intermolecular potential given by

$$V(x) = 4\epsilon(x^{-12} - x^{-6}) \quad (4-36)$$

Here  $\epsilon$  is the depth of the potential and  $x=R/\sigma$ . For intermediate temperatures, the pair distribution function  $g_0(x)$  can be expanded as an asymptotic series in powers of the Planck's constant,  $h$ . The resulting expressions for  $\mathbf{I}$  and  $\mathbf{J}$  are given by Van Kranendonk and

Kiss (1959) in the form

$$\mathbf{I} = \mathbf{I}_{C\ell} - \Lambda^{*2} \mathbf{I}^{(2)} + \Lambda^{*4} \mathbf{I}^{(4)} + \dots \quad (4-37)$$

$$\mathbf{J} = \mathbf{J}_{C\ell} - \Lambda^{*2} \mathbf{J}^{(2)} + \Lambda^{*4} \mathbf{J}^{(4)} + \dots \quad (4-38)$$

where

$$\Lambda^* = (h^2/2m_{00}\epsilon\sigma^2)^{\frac{1}{2}} \quad (4-39)$$

is the reduced mean de Broglie wave length,  $m_{00}$  being the reduced mass of the colliding pair of molecules. The numerical values  $\mathbf{I}_{C\ell}$ ,  $\mathbf{I}^{(2)}$ ,  $\mathbf{I}^{(4)}$ ,  $\mathbf{J}_{C\ell}$ ,  $\mathbf{J}^{(2)}$ , and  $\mathbf{J}^{(4)}$  for pure hydrogen using the ratio  $\rho/\sigma = 0.126$  have been evaluated by Van Kranendonk and Kiss (1959) for reduced temperatures  $T^*(=kT/\epsilon)$  from 1 to 10. As suggested by Van Kranendonk (1958), we now assume that  $\rho/\sigma$  has the same value for all the mixtures as the one for hydrogen because the temperature dependence of  $\tilde{\alpha}_{1b}$  has not been determined experimentally with sufficient accuracy. This assumption enables one to make use of the values of  $\mathbf{I}_{C\ell}$ ,  $\mathbf{I}^{(2)}$ ,  $\mathbf{I}^{(4)}$ ,  $\mathbf{J}_{C\ell}$ ,  $\mathbf{J}^{(2)}$ , and  $\mathbf{J}^{(4)}$  of pure hydrogen, mentioned above, for the mixtures as well. The interpolated values of  $\mathbf{I}$  and  $\mathbf{J}$  for the mixtures and the corresponding values of  $T^*$  for  $T=298^{\circ}\text{K}$ , and  $\Lambda^*$ , calculated from (4-39) are summarized in Table IV. The values of  $\sigma(=\frac{1}{2}(\sigma_1+\sigma_2))$  and  $\epsilon(=(\epsilon_1\epsilon_2)^{\frac{1}{2}})$  are also given in Table IV which contains the values of  $\tilde{\gamma}$ , as well, calculated from eq.(4-28). The values of the quadrupole moment,  $Q$  and the average polarizability,  $\alpha$ , of the perturbing gases and those of the rates of change of quadrupole moment and polarizability with respect to the internuclear distance,  $Q'$  and  $\alpha'$ , respectively, of the absorbing gas (hydrogen) are included in the same Table.

TABLE IV

Molecular data used in the analysis of the binary absorption coefficients of the induced fundamental band of hydrogen

Mixture	$\sigma^a$ ( $\text{\AA}^2$ )	$\epsilon/k^a$ ( $^{\circ}\text{K}$ )	$T^*$	$\Lambda^*$	<b>I</b>	<b>J</b>	$\tilde{\nu} \times 10^{32}$ ( $\text{cm}^6 \text{sec}^{-1}$ )	$Q/ea_0^2$	$Q'/ea_0$	$\alpha/a_0^3$	$\alpha'/a_0^2$
H <sub>2</sub> -H <sub>2</sub>	2.928	37.00	8.05	1.738	4.04	12.96	5.80	0.49 <sup>b</sup>	0.51 <sup>c</sup>	5.44 <sup>d</sup>	3.9 <sup>d</sup>
H <sub>2</sub> -He	2.742	19.45	15.32	2.215	6.35	15.22	4.76	0	-	1.4 <sup>e</sup>	-
H <sub>2</sub> -Ne	2.839	36.29	8.21	1.342	4.06	13.14	5.29	0	-	2.7 <sup>e</sup>	-
H <sub>2</sub> -A	3.167	66.59	4.48	0.868	2.84	12.11	7.34	0	-	11.1 <sup>e</sup>	-
H <sub>2</sub> -Kr	3.264	79.54	3.75	0.761	2.63	11.90	8.04	0	-	16.8 <sup>e</sup>	-
H <sub>2</sub> -N <sub>2</sub>	3.313	59.30	5.02	0.888	3.04	12.23	8.40	1.1 <sup>f</sup>	-	11.95 <sup>g</sup>	-
H <sub>2</sub> -O <sub>2</sub>	3.254	65.94	4.52	0.854	2.87	12.09	7.96	0.22 <sup>h</sup>	-	10.79 <sup>g</sup>	-
H <sub>2</sub> -Xe	3.514	90.42	3.30	0.660	2.48	11.92	10.03	0	-	27.4 <sup>e</sup>	-

<sup>†</sup> $Q$  and  $\alpha$  refer to the perturbing molecules only;  $a_0 = 0.529 \text{\AA}$ , Bohr radius; **I** and **J** are derived from the data obtained for Hydrogen by Van Kranendonk, J. and Kiss, Z. J. 1959. Can. J. Phys. 37, 1187.

<sup>a</sup> $\sigma$  and  $\epsilon/k$  for the mixtures are obtained from those of the component gases as given by Hirschfelder, J.O., Curtis, F.C., and Bird, R.B., 1954. Molecular Theory of Gases and Liquids (Wiley, New York).

<sup>b</sup>Poll, J. D. and Van Kranendonk, J. 1962. Can. J. Phys. 40, 163.

<sup>c</sup>See Chapter V of this thesis.

<sup>d</sup>See Hunt, J. L. and Welsh, H.L. 1964. Can. J. Phys. 42, 873.

<sup>e</sup>See Van Kranendonk, J. 1958, Physica 23, 825.

<sup>f</sup>Reddy, S. P. and Cho, C. W. 1965, Can. J. Phys. 43, 2331

<sup>g</sup>Bridge, N. J. and Buckingham, A.D. 1964. J. Chem Phys 40, 2733.

<sup>h</sup>Buckingham, A.D. Private Communication.

The quadrupole part  $(\mu_1^2 + \mu_2^2) \mathbf{J} \tilde{\gamma}$  of the total binary absorption coefficient in eq. (4-34) for each of the mixtures  $H_2-H_2$ ,  $H_2-He$ ,  $H_2-Ne$ ,  $H_2-A$ ,  $H_2-Kr$ , and  $H_2-N_2$  is calculated first, using the parameters given in Table IV, and eqs. (4-25) and (4-26) for  $\mu_1$  and  $\mu_2$  respectively. The overlap part  $\lambda^2 \mathbf{I} \tilde{\gamma}$  is then obtained by subtracting the quadrupole part from  $\tilde{\alpha}_{1a}$  for pure hydrogen, and from  $\tilde{\alpha}_{1b}$  for the corresponding mixture. Next,  $\lambda^2$  and hence  $\lambda$  are estimated. The results of these calculations and the percentage contributions of the overlap and quadrupole parts of the binary absorption coefficients for each of the mixtures are summarized in Table V. From this Table, we notice that the overlap part contributes 94% and 92% respectively in  $H_2-He$  and in  $H_2-Ne$  mixtures. The overlap part for  $H_2-N_2$  contributes only 50%.

One would naturally expect that there is a close relationship between the value of the induced moment at a distance  $R=\sigma$ , the intermolecular distance for which the potential  $V(R)=0$  and  $\epsilon$ , the minimum energy of attraction or the depth of the potential well in the Lennard-Jones potential (eq. 4-36). The values of  $\lambda$  for the mixtures  $H_2-He$ ,  $H_2-H_2$ ,  $H_2-Ne$ ,  $H_2-N_2$ ,  $H_2-A$  and  $H_2-Kr$  from Table V are plotted against the corresponding values  $\epsilon/k$ , given in Table IV. It is very interesting to note that there is an exact linear relationship between the values of  $\lambda$  and  $\epsilon$ . Using the linear relationship obtained in Fig. 9, the values of  $\lambda$  for  $H_2-O_2$  and  $H_2-Xe$  in which the infrared fundamental band of hydrogen has not been studied experimentally are obtained, ( $\lambda = 11.5 \times 10^{-3}$  for  $H_2-O_2$  and  $14.3 \times 10^{-3}$  for  $H_2-Xe$ ). Then using the molecular parameters for these two mixtures, given in Table IV,

TABLE V

Electron overlap and molecular quadrupole parts of the binary absorption coefficients

Mixture	Binary absorption coefficients		Quadrupole part	Overlap part	$\lambda^2 \times 10^5$	$\lambda \times 10^3$	Percentage	
	$(\text{cm}^{-2}\text{Amagat}^{-2})$ $\times 10^3$	$(\text{cm}^6\text{sec}^{-1})$ $\times 10^{35}$	$(\mu_1^{-2} + \mu_2^{-2}) \mathbf{J} \bar{\nu}$ $\times 10^{35}$ $(\text{cm}^6\text{sec}^{-1})$	$\lambda^2 \mathbf{I} \bar{\nu} \times 10^{35}$ $\text{cm}^6\text{sec}^{-1}$			Overlap	Quad.
H <sub>2</sub> -H <sub>2</sub>	$\alpha_{1a}:2.4$	$\bar{\alpha}_{1a}:2.27$	1.03	1.24	5.36	7.32	55	45
H <sub>2</sub> -He	$\alpha_{1b}:1.1$	$\bar{\alpha}_{1b}:1.03$	0.06	0.97	3.24	5.69	94	6
H <sub>2</sub> -Ne	2.50	2.37	0.18	2.19	10.3	10.14	92	8
H <sub>2</sub> -A	4.1	3.86	1.70	2.16	10.5	10.24	56	44
H <sub>2</sub> -Kr	8.02	7.56	3.32	4.24	20.3	14.22	56	44
H <sub>2</sub> -N <sub>2</sub>	5.4	5.11	2.58	2.53	10.0	10.0	50	50

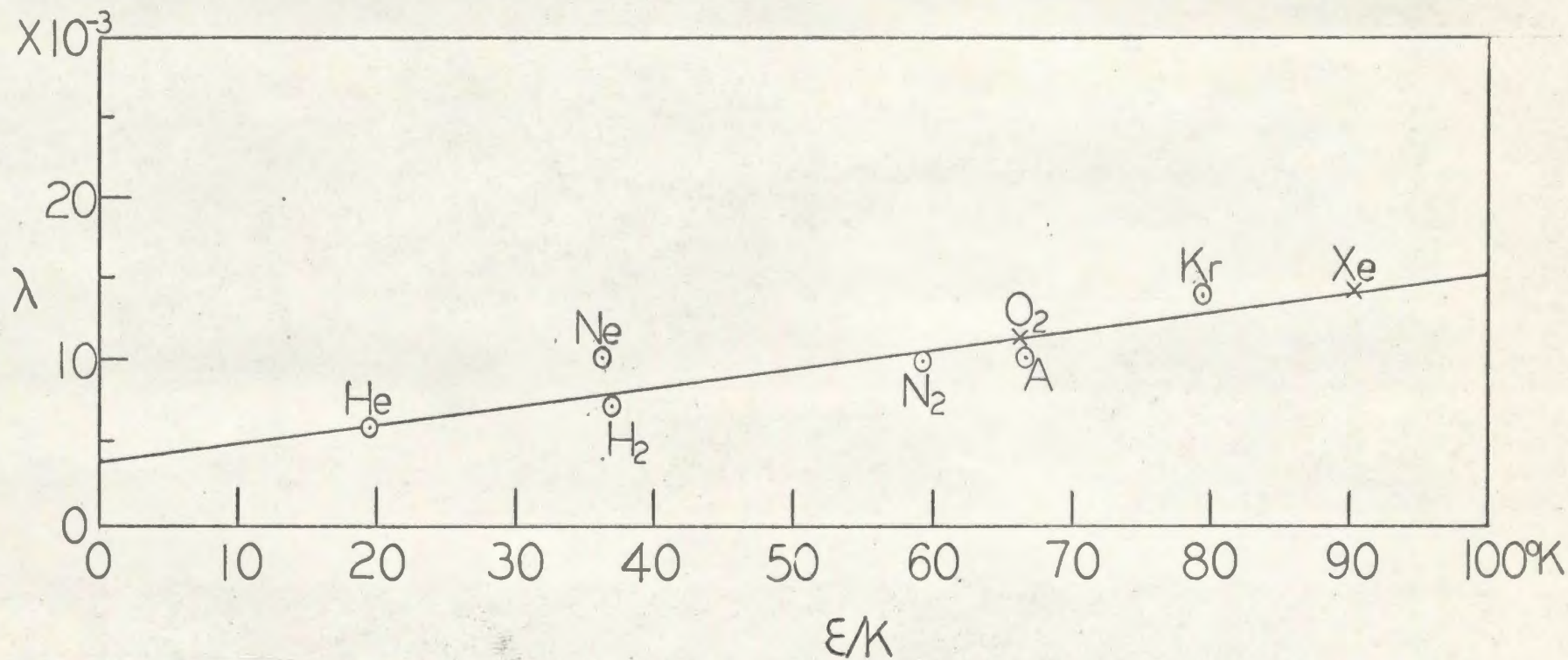


Fig. 9 The overlap parameter  $\lambda$  as a function of the temperature  $\epsilon/k$  for hydrogen-foreign gas mixtures. The crosses give the predicted values of  $\lambda$  for H<sub>2</sub>-O<sub>2</sub> and H<sub>2</sub>-Xe mixtures.

the overlap parts  $\lambda^2 \mathbf{I} \tilde{\gamma}$  and the quadrupole parts  $(\mu_1^2 + \mu_2^2) \mathbf{J} \tilde{\gamma}$  are calculated. The resulting predicted values of the binary absorption coefficients for these mixtures are obtained as follows:

$$\tilde{\alpha}_{1b} = 4.45 \times 10^{-35} \text{cm}^6 \text{sec}^{-1} (\text{i.e. } \alpha_{1b} = 4.7 \times 10^{-3} \text{cm}^{-2} \text{Amagat}^{-2})$$

for  $\text{H}_2\text{-O}_2$

$$\tilde{\alpha}_{1b} = 11.23 \times 10^{-35} \text{cm}^6 \text{sec}^{-1} (\text{i.e. } \alpha_{1b} = 11.8 \times 10^{-3} \text{cm}^{-2} \text{Amagat}^{-2})$$

for  $\text{H}_2\text{-Xe}$

It will be interesting to verify these predictions experimentally. However, one must be cautious in doing experiments with  $\text{H}_2\text{-O}_2$  mixtures because of their possible violent reaction under high pressure.

Finally the binary absorption coefficients of the individual lines of the O and S branches and the quadrupole part of the Q branch are calculated using eqs. (4-19) to (4-21) for  $\text{H}_2\text{-H}_2$  and eqs. (4-22) to (4-24) for mixtures  $\text{H}_2\text{-He}$ ,  $\text{H}_2\text{-Ne}$ ,  $\text{H}_2\text{-Ar}$ ,  $\text{H}_2\text{-Kr}$  and  $\text{H}_2\text{-N}_2$ . The results are summarized in Table VI. For the purpose of comparison, the recalculated values of the total binary absorption coefficients and the values of the overlap parts of the Q branch, are included in the same Table.

In the above calculations, the normalized Boltzmann factors  $P(J)$  occurring in eqs. (4-19) to (4-24) for various rotational levels have been obtained by eq. (4-32) using the rotational constant  $B_0 = 59.339 \text{ cm}^{-1}$ , of hydrogen as given by Stoicheff (1957).

TABLE VI

Binary absorption coefficients of the fundamental band of hydrogen ( $10^{-35}\text{cm}^6\text{sec}^{-1}$ )

Mixture	0(3)	0(2)	$Q_{\text{overlap}}$	$Q_{\text{quad.}}$	S(0)	S(1)	S(2)	S(3)	Total
H <sub>2</sub> -H <sub>2</sub>	0.01	0.02	1.24	0.59	0.08	0.26	0.04	0.03	2.27
H <sub>2</sub> -He	-	-	0.97	0.02	0.01	0.03	-	-	1.03
H <sub>2</sub> -Ne	-	-	2.19	0.06	0.02	0.08	0.01	0.01	2.37
H <sub>2</sub> -A	0.04	0.04	2.16	0.55	0.22	0.68	0.10	0.07	3.86
H <sub>2</sub> -Kr	0.08	0.08	4.24	1.07	0.43	1.32	0.20	0.14	7.56
H <sub>2</sub> -N <sub>2</sub>	0.04	0.04	2.53	1.48	0.21	0.64	0.10	0.07	5.11

CHAPTER V

ANALYSIS OF THE ABSORPTION PROFILES OF  
THE PRESSURE INDUCED INFRARED FUNDAMENTAL BAND OF  
HYDROGEN IN H<sub>2</sub>-Ne AND H<sub>2</sub>-Kr MIXTURES

5.1 Introduction:

As noted earlier, homonuclear diatomic gases which normally do not absorb radiation at their vibrational and rotational frequencies can be made to absorb radiation when they or their mixtures with foreign gases are compressed. This phenomenon occurs as a result of the dipole moment induced in the molecules of these diatomic gases during molecular collisions. The induced absorption is mainly produced by binary collisions between the absorbing molecules and the perturbing molecules. Only at high pressures, ternary and higher order collisions contribute a considerable amount to the total absorption. At moderate pressure the absorption lines maintain almost constant shape. One of the main characteristics of the pressure induced absorption spectra is their broad diffuse appearance which is due to the participation of the relative translational energy of the colliding pairs of molecules in the absorption process. This participation causes a line of molecular frequency  $\nu_0$  to have a frequency distribution consisting of summation and difference tones,  $\nu_0 \pm \nu_k$ , where  $\nu_k$  is the continuum of frequencies that is exchanged by the absorbing and the perturbing molecules in the duration of the collision process. Due to the effect of  $\nu_k$ , the induced infrared fundamental band of hydrogen at room temperature actually extends over more than  $2000 \text{ cm}^{-1}$  with a few broad maxima at the positions of its vibrational and vibrational-rotational frequencies.

By a careful analysis of the profiles of the induced infrared absorption spectra, it is possible to obtain information about the extent of the individual lines of the band, their shape etc. Under favorable conditions it will be also possible to obtain the values of the molecular constants such as quadrupole moment, its derivative with respect to the internuclear axis in the equilibrium position, etc. from such an analysis. In this chapter we give details of the analysis of the profiles of the induced infrared fundamental band of hydrogen obtained in H<sub>2</sub>-Ne and H<sub>2</sub>-Kr mixtures at room temperature. Before doing so, it is worthwhile to present a brief survey of the work done on the band profiles of hydrogen by earlier investigators.

## 5.2 Previous Work on Band Profiles of Hydrogen:

### (i) The rotational-translational absorption spectrum of hydrogen:

Kiss and Welsh (1959) studied the rotational-translational pressure-induced absorption spectrum of hydrogen and found that the profile of an individual rotational line is asymmetric with the intensity degraded towards higher frequencies. They also found an analytical expression that reproduced the observed line shapes very well, except in the high frequency wings. This is the dispersion line shape modified by the Boltzmann law which can be expressed as:

$$\begin{aligned} \tilde{\alpha}(\nu) &= \frac{\tilde{\alpha}^0}{1 + \left(\frac{\nu - \nu_0}{\delta}\right)^2}, & \nu > \nu_0 \\ &= \frac{\tilde{\alpha}^0}{1 + \left(\frac{\nu - \nu_0}{\delta}\right)^2} \exp(-hc\Delta\nu/kT), & \nu < \nu_0 \end{aligned} \tag{5-1}$$

where  $\bar{\alpha}^0$  is the peak intensity (free from the frequency-dependent factor) at the origin,  $\nu_0$ , of the line,  $\bar{\alpha}(\nu)$  is the intensity at frequency  $\nu$  and is given by  $(1/\nu\ell)\log_e(I_0(\nu)/I(\nu))$ ,  $\delta$  is a half-width parameter of the line profile and is equal to the value of  $\nu - \nu_0$  for  $\nu > \nu_0$  where  $\bar{\alpha}(\nu)$  is  $\bar{\alpha}^0/2$  and  $\Delta\nu = |\nu - \nu_0|$ . The quantity  $\ell$  is the length of the absorption cell in centimeters,  $I_0(\nu)$  is the intensity of light incident on the gas and  $I(\nu)$  is the intensity of the light transmitted by the gas. The measurements of Kiss and Welsh (1959) were limited to about  $350 \text{ cm}^{-1}$  on the low frequency side. Bosomworth and Gush (1965) studied the same absorption spectrum of hydrogen and were able to reach down to a frequency of about  $20 \text{ cm}^{-1}$ . They found that the dispersion line shape gave too much intensity in the tails of an individual line. A much better fit was obtained when the tail of the line was represented in an exponential form:

$$\begin{aligned} \bar{\alpha}(\nu) &= \frac{\bar{\alpha}^0}{1 + \left(\frac{\nu - \nu_0}{\delta}\right)^2}, & \nu_0 \leq \nu \leq \nu_0 + 1.5\delta, \\ &= C \exp(-D \Delta\nu), & \nu > \nu_0 + 1.5\delta, \\ &= \frac{\bar{\alpha}^0}{1 + \left(\frac{\nu - \nu_0}{\delta}\right)^2} \exp(-hc\Delta\nu/kT), & \nu_0 - 1.5\delta \leq \nu \leq \nu_0, \\ &= C \exp(-D \Delta\nu) \exp(-hc\Delta\nu/kT), & \nu < \nu_0 - 1.5\delta \end{aligned} \quad (5-2)$$

Here C and D are constants that allow the exponential "tail" to be joined smoothly to the dispersion line profile. The Boltzmann factor modifying the line shape for frequencies  $\nu < \nu_0$  accounts for the thermal distribution of the excited translational states.

(ii) The pressure-induced fundamental band of hydrogen:

Hunt and Welsh (1964) analysed for the first time the profile

of the fundamental band of hydrogen in pressure-induced absorption in the pure gas and in  $H_2$ -He mixtures at  $300^\circ K$ ,  $195^\circ K$ , and  $78^\circ K$ , and in  $H_2$ -A and  $H_2$ - $N_2$  mixtures at  $300^\circ K$ . In their computational procedure for the analysis of the profiles, they assumed, for the sake of simplicity, the overlap part of the Q branch would consist of only the  $Q_{\text{overlap}}(1)$  line. They considered the contributions of the quadrupole lines  $Q_{\text{quad}}(1)$  and  $S(J)$ ,  $J=0, 1, 2$ , and  $3$ . For the contours obtained in pure hydrogen, they considered possible strong double transitions of the  $S(J)$  lines in addition to the usual single transitions. Following the observations of Kiss and Welsh (1959) on the profiles of the rotational-translational spectrum of hydrogen, Hunt and Welsh (1964) assumed dispersion line shapes modified by Boltzmann law both for the overlap  $Q(1)$  line and for the individual quadrupole lines.

Gush, Nanassy and Welsh (1957) explained the doublet structure in the  $Q_p$  component of the Q branch by the consideration that each of the individual components of the Q branch i.e.  $Q(0)$ ,  $Q(1)$ ,  $Q(2)$  and  $Q(3)$  has a doublet structure with the components  $Q_p$  and  $Q_R$ .

### 5.3 Method of Analysis of the Profiles Obtained in the Present Work

(i) The composition of the enhancement absorption profiles of the fundamental band of hydrogen in  $H_2$ -Ne and  $H_2$ -Kr mixtures.

The fundamental band of hydrogen consists of three types of transitions: the selection rule  $\Delta J = 0$  gives  $Q(J)$  transitions while  $\Delta J = +2$  and  $-2$  give  $S(J)$  and  $O(J)$  transitions respectively. In the band obtained with pure hydrogen gas, the S lines induced in  $H_2$ - $H_2$

collisions occur as single as well as double transitions (Hunt and Welsh, 1964). In a double transition, one of the colliding pair of  $H_2$  molecules makes a vibrational transition  $\Delta v = 1$  while the other makes a rotational transition  $\Delta J = 0, \pm 2$ . On the other hand, the enhancement absorption profiles of the band in hydrogen-foreign gas binary mixtures exclusively contain single transitions. In a single transition, the absorbing molecule of the colliding pair of molecules makes the vibration-rotation transition  $\Delta v = 1; \Delta J = 0, \pm 2$ , while the internal energy of the perturbing molecule remains unchanged. Since the energy levels of molecules in pressure-induced absorption spectrum are not perturbed and the selection rules for the induced absorption spectrum and the Raman spectrum are the same, the frequency structure of the pressure-induced infrared fundamental band of hydrogen in absorption are considered to be the same as that of the Raman fundamental band. The frequencies of transitions are calculated from the molecular constants of hydrogen derived by Stoicheff (1957) from the high resolution data of the Raman fundamental band of hydrogen obtained at low pressure. All the possible single transitions of the pressure induced fundamental band of hydrogen are summarized in Table VII.

As described in Chapter IV, the fundamental band of hydrogen arises from a short-range interaction due to electron overlap forces and a long-range interaction resulting from molecular quadrupolar induction. The overlap forces are almost independent of relative orientation of the colliding pairs of molecules and contribute a major portion to the intensity of the Q transitions. The experimentally observed splitting of the Q branch into two parts designated as  $Q_p$  (on

TABLE VII

Frequencies of single transitions in H<sub>2</sub> fundamental band

Line	Frequency	Remarks
O(3)	3568.3 cm <sup>-1</sup>	Quadrupolar
O(2)	3806.7 "	"
Q(3)	4125.8 "	Quadrupolar (Q <sub>Q</sub> ) and overlap Q <sub>R</sub> , Q <sub>P</sub>
Q(2)	4143.4 "	" and "
Q(1)	4155.2 "	" and "
Q(0)	4161.1 "	Overlap (Q <sub>R</sub> , Q <sub>P</sub> )
S(0)	4497.7 "	Quadrupolar
S(1)	4712.8 "	"
S(2)	4907.4 "	"
S(3)	5109.0 "	"

the low frequency side) and  $Q_R$  (on the high frequency side) as well as the small splitting of  $Q_P$  itself in some cases (for example in the enhancement contours in  $H_2$ -Ne mixtures at low pressures), is considered to be the result of the splittings of the individual components  $Q_{\text{overlap}}(J)$  of the overlap part of the Q branch for possible values of J into their respective components  $Q_P(J)$  and  $Q_R(J)$ . The long-range quadrupolar interaction is, on the other hand, strongly dependent on the relative orientation of the colliding pair of molecules and is responsible for most of the intensity of the O and S transitions and a part of the intensity of the Q transition. The quadrupolar component of the Q branch is designated as  $Q_Q$  and its existence has been experimentally shown in pure  $H_2$  and in  $H_2$ -A and  $H_2$ - $N_2$  mixtures, at high pressures, by Hare and Welsh (1958) and in  $H_2$ -Kr mixtures at moderate pressures in the present investigation. The  $Q_Q$  component is not resolved at low pressures.

Thus the enhancement contours of the fundamental band of hydrogen at room temperature are considered to consist of the following thirteen components: O(J), J=2 and 3,  $Q_{\text{overlap}}(J)$  and S(J), J=0, 1, 2 and 3;  $Q_Q(J)$ , J=1, 2 and 3. In the  $Q_Q$  branch, the line  $Q_Q(0)$  does not occur because the transition  $J'=0 \leftarrow J''(=J)=0$  is forbidden for a quadrupolar branch. The relative peak heights of all these thirteen lines were taken from the formula given by Van Kranendonk (1958).

(ii) Line-shape used in obtaining synthetic profiles; and analysis of the profiles:

In the present analysis of the enhancement profiles of the hydrogen fundamental band obtained in  $H_2$ -Ne and  $H_2$ -Kr mixtures, the

modified dispersion line shape with an exponential tail considered by Bosomworth and Gush (1965) in obtaining a synthetic profile that fits the pure rotational spectrum of hydrogen has been used with a slight modification. The shape of an individual vibration-rotation line is therefore represented by equations (5-2). The only modification is that an exponential tail occurs beyond  $\Delta\nu = \nu - \nu_0 = 1.75\delta$ , instead of  $1.5\delta$ . Actually several trial values for this  $\Delta\nu$  ranging from  $1.5\delta$  to  $5.0\delta$  were used but the consideration that the exponential tail occurs beyond  $\Delta\nu = 1.75\delta$  gave the best fit of the synthetic profiles with the experimental profiles.

The half-widths  $\delta_Q$  of the four overlap lines  $Q_{\text{overlap}}(J)$ ,  $J = 0, 1, 2, 3$  were assumed to be the same; similarly the half-widths  $\delta_S$  of the nine quadrupolar lines were also assumed to be equal. The peak intensities of the overlap lines were expressed as fractions of the peak intensity of the strongest overlap line at room temperature i.e.  $Q_{\text{overlap}}(1)$ . Similarly, the peak intensities of the quadrupolar lines were expressed in terms of that of the  $S(1)$  line.

Finally a trial-and-error method was used in fitting the resultant of the calculated distributions of all the individual lines to the experimental profiles. Reasonable values were assumed for the  $\delta_Q$  and  $\delta_S$  and the resultant of the calculated intensity distributions was matched to the experimental enhancement profile both in the high and low frequency sides of the band origin to give values of  $\bar{\alpha}_{Q(1)}^0(\text{overlap})$  (hereafter written without the words in parenthesis) and  $\bar{\alpha}_{S(1)}^0$ . Thus, by a successive choice of  $\delta_Q$  and  $\delta_S$ , a set of values  $\bar{\alpha}_{Q(1)}^0$ ,  $\delta_Q$ ;  $\bar{\alpha}_{S(1)}^0$  and  $\delta_S$  giving the best fit of the resultant synthetic profile

with the experimental profile was obtained. These calculations were carried out using the IBM 1620 computer of the Memorial University of Newfoundland.

#### 5.4 Results and Discussion:

The result of the analysis described in the previous section is shown in Fig.10 for an enhancement absorption profile obtained for a H<sub>2</sub>-Ne mixture at 298<sup>0</sup>K with  $\rho_{H_2} = 48.7$  amagat and  $\rho_{Ne} = 109.5$  amagat. The experimental profile is represented by the solid curve. The dashed curves are the quadrupolar O, S and Q<sub>0</sub> and the overlap Q<sub>p</sub> and Q<sub>R</sub> components. The sum of these dashed curves gives the computed contour which gives the best fit to the experimental contour. To maintain clarity of the profiles of these quadrupolar and overlap branches, the profiles of the individual lines are not shown in Fig.10. It is clear that the agreement between the calculated and experimental profiles both on the high and low frequency wings is very satisfactory. The apparent disagreement between the experimental and calculated profiles in the neighborhood of the band origin is due to the splitting of the Q branch into the Q<sub>p</sub> and Q<sub>R</sub> components. A similar but small disagreement between these near the S(1) peak is due to the splitting of the S(1) line which is due to the contribution of a considerable amount of overlap interaction to this line. Profile analyses were similarly made for several other enhancement contours of the hydrogen fundamental band obtained in H<sub>2</sub>-Ne mixtures with different base densities of hydrogen and several densities of neon. ( $\rho_{H_2}=37.6$  Amagat with  $\rho_{N_2}=36.6, 69.2, 98.8, 152.5, 180.5, 199.8, 224.1$  and  $242.9$  Amagat;

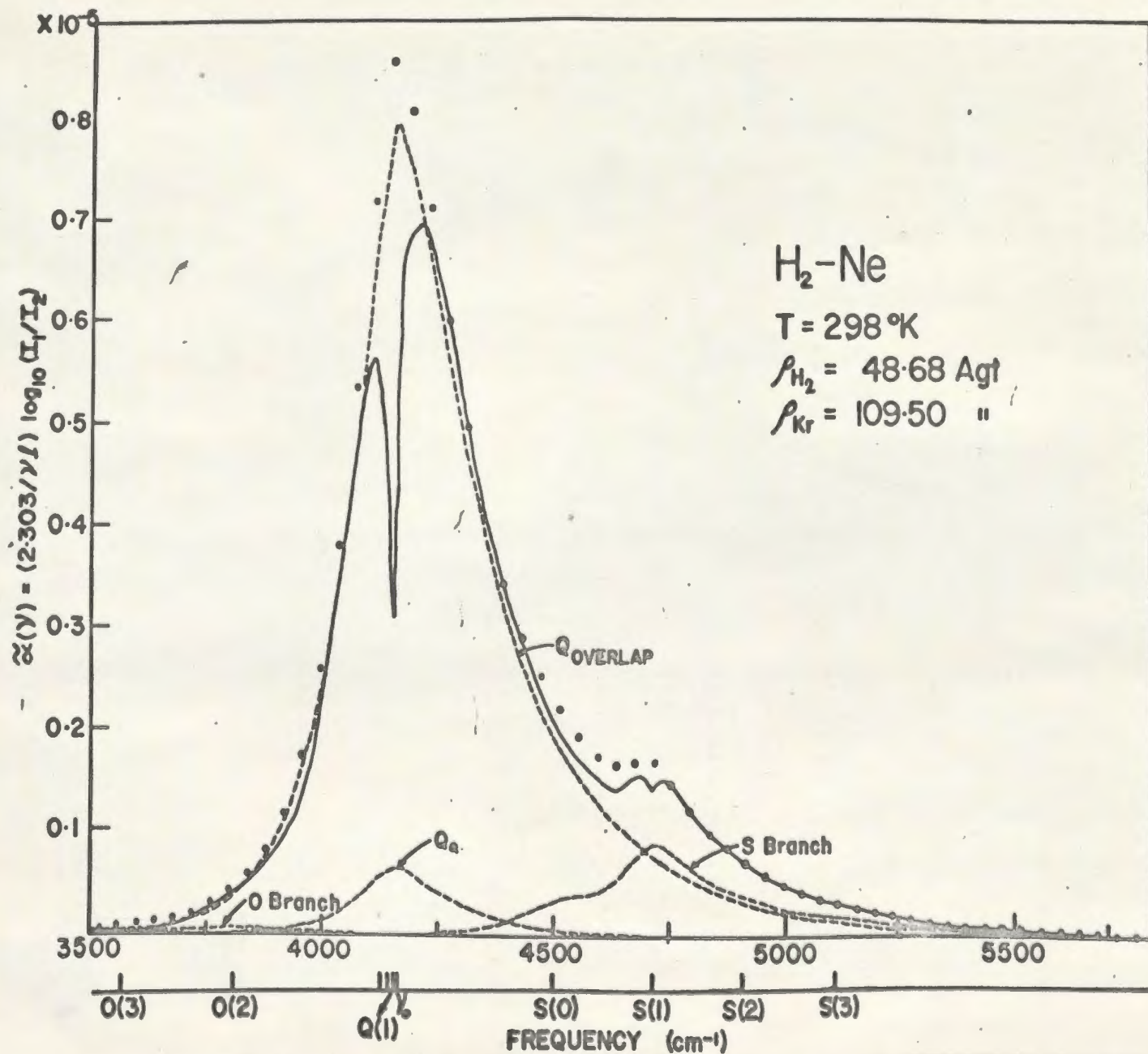


Fig. 10 Analysis of the enhancement absorption profile of the hydrogen fundamental band in a hydrogen-neon mixture. The dashed profiles indicate the overlap Q component and the quadrupolar O,  $Q_0$  and S components obtained from the analysis and the dots the resultant of these. The solid contour is the experimental profiles.

$\rho_{H_2} = 45.0$  Amagat with  $\rho_{Ne} = 32.3, 57.0, 81.4, 126.5, 152.0$  and  $177.0$  Amagat; and  $\rho_{H_2} = 48.7$  Amagat with  $\rho_{Ne} = 31.0, 57.3, 84.3, 159.5, 185.7, 207.7$  and  $228.7$  Amagat.) The values obtained for  $\delta_Q$  and  $\delta_S$  were  $200 \pm 10 \text{ cm}^{-1}$  and  $130 \pm 5 \text{ cm}^{-1}$  respectively (Table VIII). The half-widths obtained were found to be independent of the gas density within the range of error quoted here.

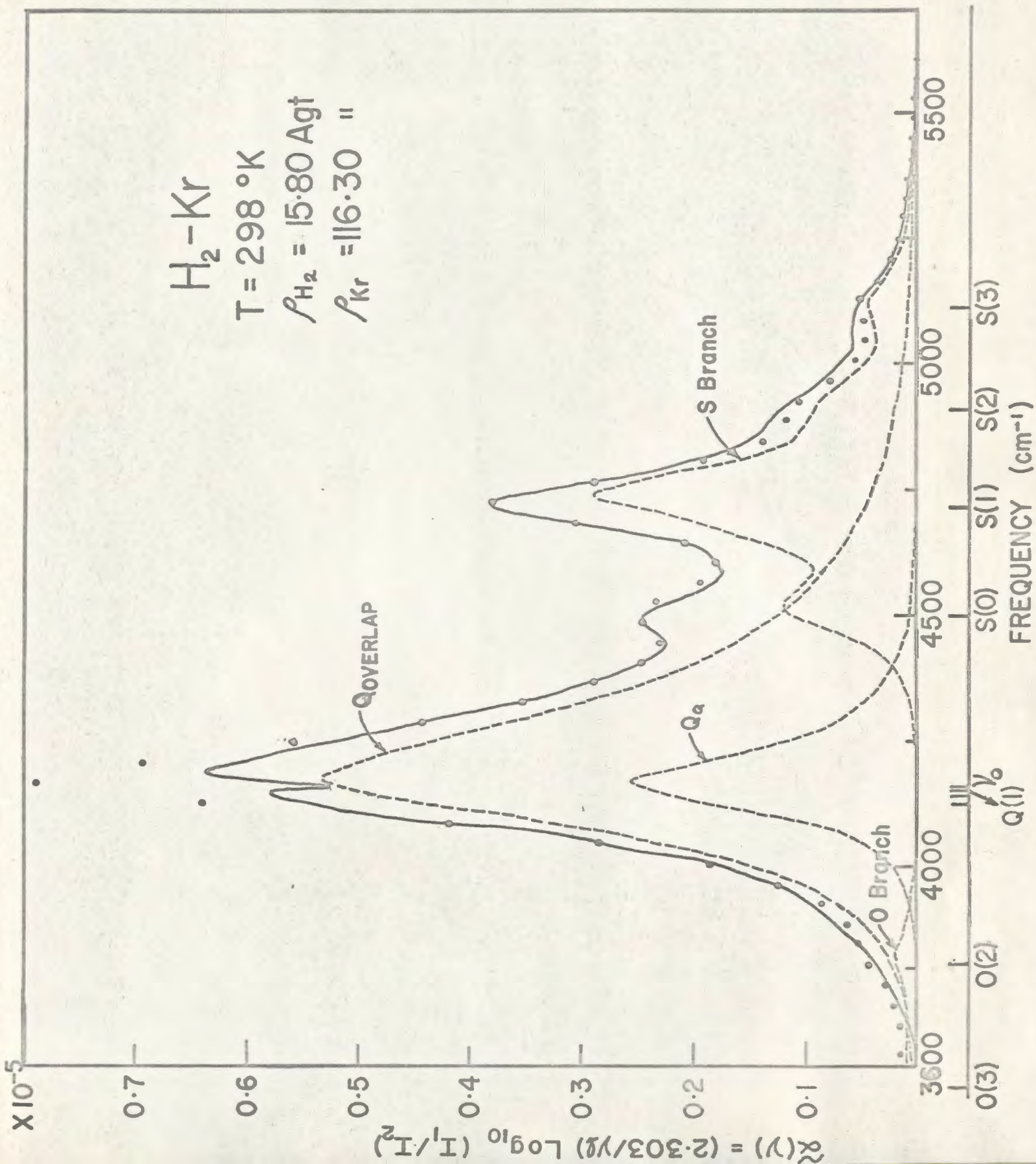
Table VIII

The values of the half-widths  $\delta_Q$  and  $\delta_S$ .

	$\delta_Q \text{ (cm}^{-1}\text{)}$	$\delta_S \text{ (cm}^{-1}\text{)}$
H <sub>2</sub> -Ne	$200 \pm 10$	$130 \pm 5$
H <sub>2</sub> -Kr	$190 \pm 10$	$78 \pm 2$

The result of a similar analysis for the enhancement absorption profile of the band obtained for a H<sub>2</sub>-Kr mixture at 298°K with  $\rho_{H_2} = 15.8$  Amagat and  $\rho_{Kr} = 116.3$  Amagat is shown in Fig. 11. The agreement between the experimental and calculated contours over the entire region of the band, except at a small region near the band origin is extremely satisfactory. The average values obtained for  $\delta_Q$  and  $\delta_S$  for profiles at a series of densities ( $\rho_{H_2} = 12.2$  Amagat with  $\rho_{Kr} = 42.1, 90.1, 135.6$  and  $185.9$  Amagat;  $\rho_{H_2} = 14.2$  Amagat with  $\rho_{Kr} = 37.7, 71.3$  and  $116.0$  Amagat; and  $\rho_{H_2} = 15.8$  Amagat, with  $\rho_{Kr} = 61.1$  and  $159.4$  Amagat), were  $190 \pm 10 \text{ cm}^{-1}$  and  $78 \pm 2 \text{ cm}^{-1}$  respectively (Table VIII). In the contours for H<sub>2</sub>-Kr mixtures also, the half-widths were found to be independent of the density of the mixture.

Fig. 11 Analysis of the enhancement absorption profile of the hydrogen fundamental band in a hydrogen-krypton mixture. The dashed profiles indicate the overlap Q component and the quadrupolar O, Q<sub>0</sub> and S components obtained from the analysis and the dots the resultant of these. The solid contour is the experimental profile.



Just as the integrated absorption coefficient of a pressure-induced fundamental band can be expressed as a power series in the densities of the component gases of a mixture, the peak intensities of the individual lines can also be expressed as a power series in number-densities of the gases. For example, the peak intensities of  $Q_{\text{overlap}}(1)$  and  $S(1)$  can be expressed as,

$$\tilde{\alpha}_{Q_{\text{overlap}}(1)}^0 = \tilde{k}_Q \tilde{\rho}_a \tilde{\rho}_b + \tilde{l}_Q \tilde{\rho}_a \tilde{\rho}_b^2 \quad (5-3)$$

and 
$$\tilde{\alpha}_{S(1)}^0 = \tilde{k}_S \tilde{\rho}_a \tilde{\rho}_b + \tilde{l}_S \tilde{\rho}_a \tilde{\rho}_b^2 \quad (5-4)$$

The values of  $\tilde{k}_Q$  and  $\tilde{l}_Q$  for the  $Q(1)$  overlap line for  $H_2$ -Ne and  $H_2$ -Kr mixtures were obtained by plotting  $\tilde{\alpha}_{Q(1)}^0 / \tilde{\rho}_a \tilde{\rho}_b$  against  $\tilde{\rho}_b$  as shown in Fig. 12 and are given in Table IX. Similarly the values of  $\tilde{k}_S$  and  $\tilde{l}_S$  for the  $S(1)$  line in these mixtures were obtained by plotting  $\tilde{\alpha}_{S(1)}^0 / \tilde{\rho}_a \tilde{\rho}_b$  against  $\tilde{\rho}_b$  (Fig. 13) and are given in Table IX.

Table IX

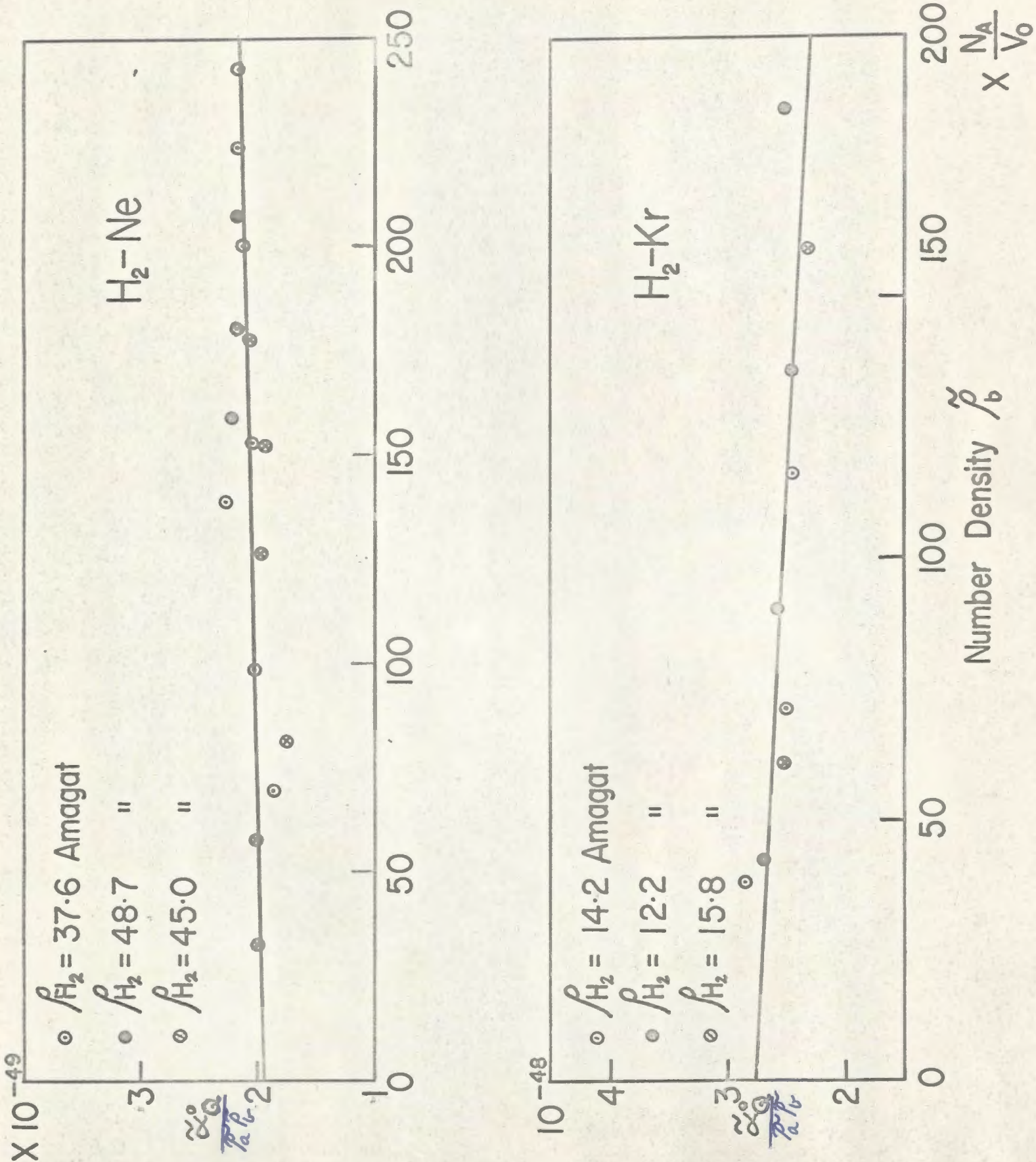
Parameters of the peak intensities of the  $Q_{\text{overlap}}(1)$  and the  $S(1)$  lines.

	$\tilde{k}_Q$	$\tilde{l}_Q$	$\tilde{k}_S$	$\tilde{l}_S$
	Agt. $\cdot^{-2} \cdot \text{cm}^6$	Agt. $\cdot^{-3} \cdot \text{cm}^6$	Agt. $\cdot^{-2} \cdot \text{cm}^6$	Agt. $\cdot^{-3} \cdot \text{cm}^6$
	$\times 10^{-48}$	$\times 10^{-71}$	$\times 10^{-48}$	$\times 10^{-70}$
$H_2$ -Ne	0.20	0.39	1.22	5.37
$H_2$ -Kr	2.78	-8.7	2.47	9.74

By using the formula

$$Q' = \left( \frac{cA\delta_S \tilde{k}_S}{J\tilde{\gamma}P(J)L_2(J, J+2)} \right)^{\frac{1}{2}} \frac{e\sigma^4}{\alpha_2} \quad (5-5)$$

Fig. 12 Relation between peak intensities of the  $Q_{\text{overlap}}(1)$  lines and the number density  $\rho_b$  of the perturbing gas.



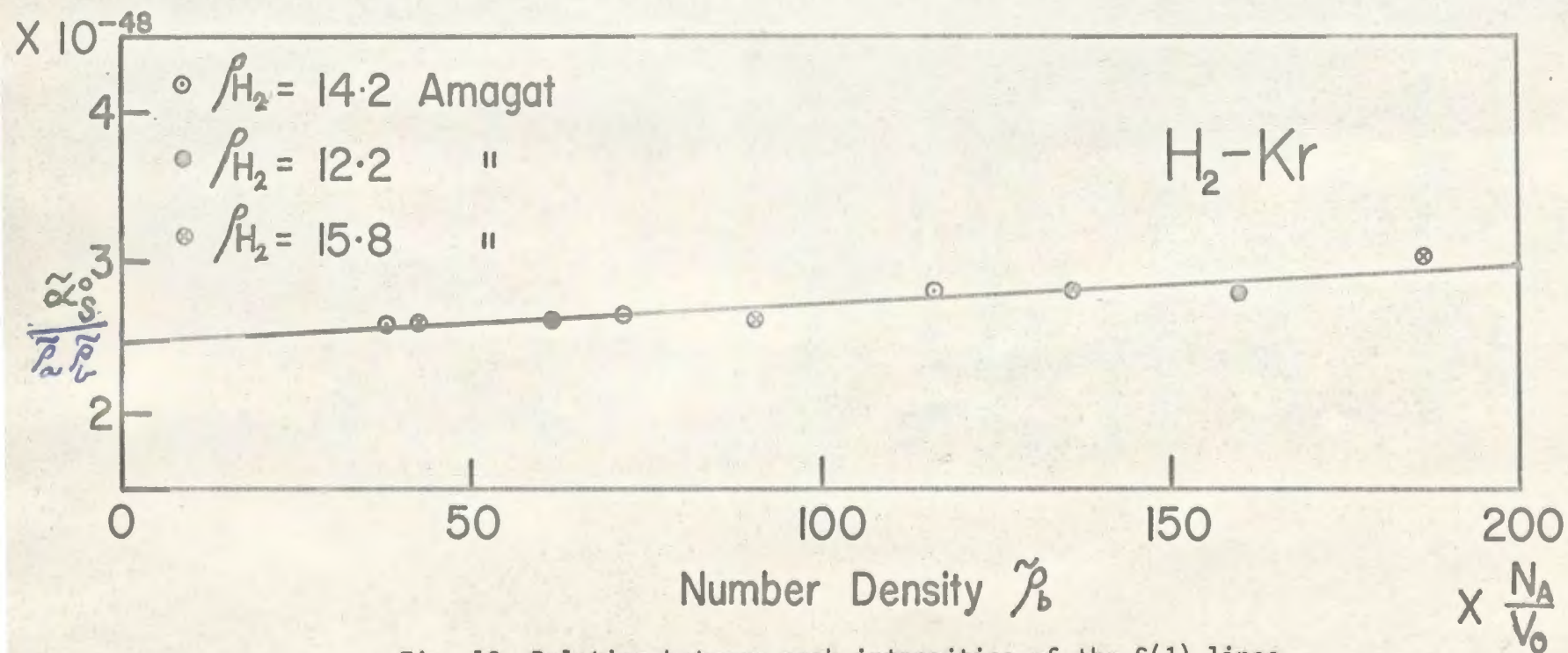
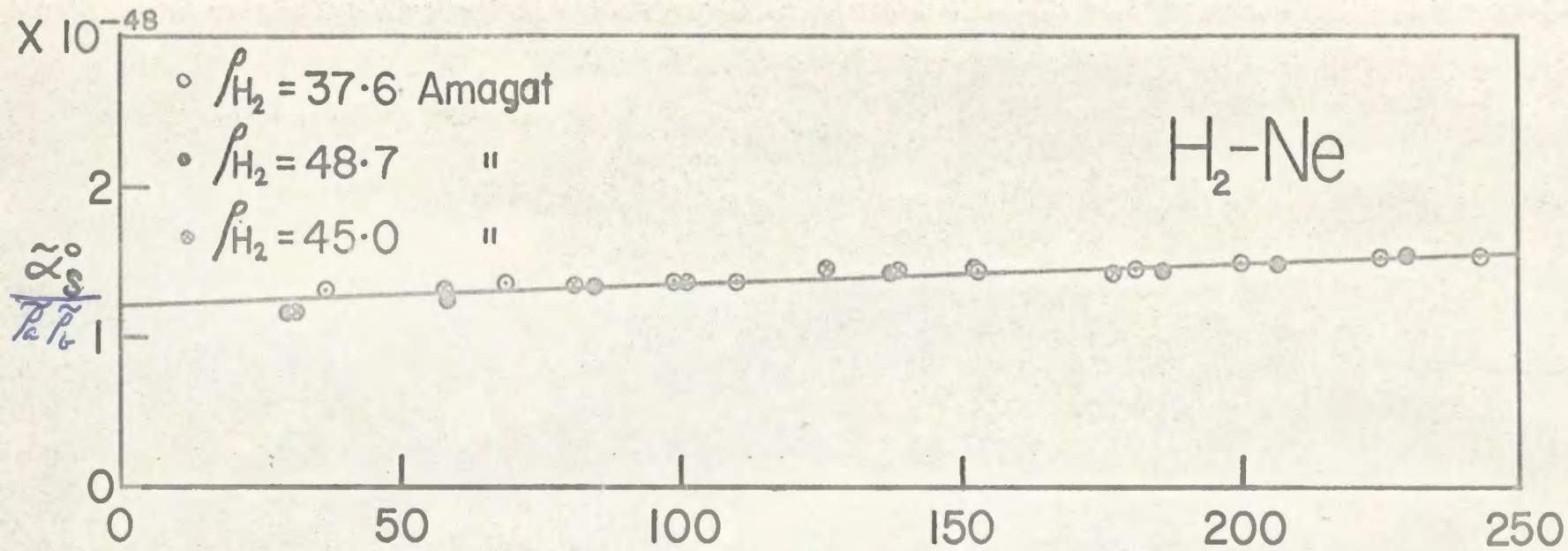


Fig. 13 Relation between peak intensities of the S(1) lines and the number density  $\tilde{\rho}_b$  of the perturbing gas.

and the value of  $\tilde{k}_S$  for the S(1) line of H<sub>2</sub>-Kr mixtures, the value of Q' for hydrogen is obtained as 0.51 ea<sub>0</sub>. The formula (5-5) is obtained from equations (4-16), (4-25), (5-4) and the explicit form of the line shape  $\tilde{\alpha}(\nu)$  used in the present analysis. Here A is the numerical integral

$$A = \frac{1}{\tilde{\alpha}_S^0 \delta_S} \int_0^\infty \tilde{\alpha}(\nu) d\nu \quad (5-6)$$

and the rotational quantum number J is equal to one.

In summary, in this chapter we have made an analysis of the enhancement absorption profiles of the fundamental band of hydrogen in H<sub>2</sub>-Ne and H<sub>2</sub>-Kr mixtures at room temperature on the lines suggested by Hunt and Welsh (1964). In doing so, the additional factors which we took into consideration are (i) the lines have a modified dispersion line shape with an exponential tail and (ii) the band consists of four overlap Q lines and nine quadrupolar lines -- three in the Q<sub>0</sub> branch, four in the S branch and two in the 0 branch.

### ACKNOWLEDGMENTS

The author is greatly indebted to his Supervisor, Dr. S.P. Reddy for his active guidance and assistance during the course of the research work and in the preparation of the thesis.

The author is grateful to Dr. S.W. Breckon for his interest in this investigation and for his encouragement.

The financial assistance received in the form of a Graduate Fellowship during the period 1965-67 from the National Research Council's operating grant A-2440, is gratefully acknowledged.

The author wishes to acknowledge the assistance received from Technical Services of Memorial University of Newfoundland, headed by Mr. W. Gordon. The use of the facilities of the Computing Centre of Memorial University of Newfoundland is also gratefully acknowledged. Mention must be made, in this connection, of the willing co-operation of Mr. J.W. Cole and <sup>Mr.</sup> J.M. Royle of Technical Services and of Mr. A. Robertson, Jr. of Computer Centre.

Thanks are gratefully extended to Messrs. W.E. Russell, A.R. Forbes, R. Bishop and S.Lagu for their assistance in preparing the diagrams and some numerical calculations.

REFERENCES

- (1) Allin, E.J., Gush, H.P., Hare, W.F.J. and Welsh, H.L. 1958. Nuovo Cimento Suppl. 9, 77.
- (2) Allin, E.J., Hare, W.F.J. and McDonald, R.E. 1955. Phys. Rev. 98, 554.
- (3) Bosomworth, D.R. and Gush, H.P. 1965. Can. J. Phys. 43, 751.
- (4) Bridge, N.J. and Buckingham, A.D. 1964. J. Chem. Phys. 40, 2733.
- (5) Briton, F.R. and Crawford, M.F. 1958. Can. J. Phys. 36, 741.
- (6) Buckingham, A.D. Private Communication.
- (7) Chisholm, D.A. and Welsh, H.L. 1954. Can. J. Phys. 32, 291.
- (8) Cho, C.W., Allin, E.J. and Welsh, H.L. 1963. Can. J. Phys. 41, 1991.
- (9) Clouter, M. and Gush, H.P. 1965. Phys. Rev. Letters 15, 200.
- (10) Crawford, M.F., Welsh, H.L. and Locke, J.L. 1949. Phys. Rev. 75, 1607.
- (11) Crawford, M.F., Welsh, H.L., McDonald, J.C.F. and Locke, J.L. 1950. Phys. Rev. 80, 469.
- (12) Colpa, J.P. and Ketelaar, J.A.A. 1958a. Mol. Physics 1, 14.
- (13) Colpa, J.P. and Ketelaar, J.A.A. 1958b. Mol. Physics 1, 343.
- (14) Condon, E.U. 1932. Phys. Rev. 41, 759.
- (15) Ewing, G.E. and Trajmar, S. 1964. J. Chem. Phys. 41, 814.
- (16) Ewing, G.E. and Trajmar, S. 1964. J. Chem. Phys. 42, 4038.
- (17) Gush, H.P., Hare, W.F.J., Allin, E.J. and Welsh, H.L. 1960. Can. J. Phys. 38, 176.
- (18) Gush, H.P. 1961. J. Phys. Rad. 22, 149.

- (19) Gush, H.P., Hare, W.F.J., Allin, E.J. and Welsh, H.L. 1957. Phys. Rev. 106, 1101.
- (20) Gush, H.P., Nanassy, A. and Welsh, H.L. 1957. Can. J. Phys. 35, 712.
- (21) Gush, H.P. and Van Kranendonk, J. 1962. Can. J. Phys. 40, 1461.
- (22) Hare, W.F.J., Allin, E.J. and Welsh, H.L. 1955. Phys. Rev. 99, 1887.
- (23) Hare, W.F.J. and Welsh, H.L. 1958. Can. J. Phys. 36, 88.
- (24) Hirschfelder, J.O., Curtis, F.C. and Bird, R.B. 1954. Molecular Theory of Gases and Liquids (Wiley, New York).
- (25) Hunt, J.L. and Welsh, H.L. 1964. Can. J. Phys. 42, 873.
- (26) Ketelaar, J.A.A., Colpa, J.P. and Hooge, F.N. 1955. J. Chem. Phys. 23, 413.
- (27) Kiss, Z.J., Gush, H.P. and Welsh, H.L. 1959. Can. J. Phys. 37, 362.
- (28) Kiss, Z.J. and Welsh, H.L. 1959. Can. J. Phys. 37, 1249.
- (29) Kudian, A. and Welsh, H.L. 1967. Bulletin of Am. Phys. Soc. Series II, Vol. 12 - BG1.
- (30) Kudian, A., Welsh, H.L. and Watanabe, A. 1965. J. Chem. Phys. 43, 3397.
- (31) Michels, A. and Goudekot, M. 1941. Physica 8, 347.
- (32) Michels, A., Wassenaar, T. and Louwerse, P. 1960. Physica 26, 539.
- (33) Pai, S.T., Reddy, S.P. and Cho, C.W. 1966. Can. J. Phys. 44, 2893.

- (34) Plyler, E.K. and Acquista, N. 1952. J. Research NBS. 49, 13.
- (35) Poll, J.D. and Van Kranendonk, J. 1961. Can. J. Phys. 39, 189.
- (36) Poll, J.D. and Van Kranendonk, J. 1962. Can. J. Phys. 40, 163.
- (37) Reddy, S.P. and Cho, C.W. 1965a. Can. J. Phys. 43, 793.
- (38) Sinha, B.B.P. 1967. M.Sc. Thesis. Memorial University of  
Newfoundland.
- (39) Sears, V.F. and Van Kranendonk, J. 1964. Can. J. Phys. 42, 980.
- (40) Stoicheff, B.P. 1957. Can. J. Phys. 35, 730.
- (41) Thomson, H.W. 1961. I.U.P.A.C. Tables of Wavenumbers, Butterworths,  
London.
- (42) Trappeniers, N.J., Wassenaar, T., and Lawerse, P.  
1966, Physica 32, 1503.
- (43) Van Kranendonk, J. and Bird. 1951. Phys. Rev. 82, 964.
- (44) Van Kranendonk, J. and Bird. 1951. Physica. 17, 953 and 968.
- (45) Van Kranendonk, J. 1952. Ph.D. Thesis. University of Amsterdam,  
Amsterdam, Netherlands.
- (46) Van Kranendonk, J. 1957. Physica. 23, 825.
- (47) Van Kranendonk, J. 1958. Physica. 24, 347.
- (48) Van Kranendonk, J. 1959. Physica. 25, 1080.
- (49) Van Kranendonk, J. 1960. Can. J. Phys. 38, 240.
- (50) Van Kranendonk, J. and Sears, V.F. 1966. Can. J. Phys. 44, 313.
- (51) Van Kranendonk, J. and Kiss, Z.J. 1959. Can. J. Phys. 37, 1187.
- (52) Watanabe, A., Kudian, A. and Welsh, H.L. 1965. JS, Symposium  
on Molecular Structure and Spectroscopy, Ohio State University.
- (53) Watanabe, A. and Welsh, H.L. 1964. Phys. Rev. Letters 13, 810.
- (54) Watanabe, A. and Welsh, H.L. 1965. Can. J. Phys. 43, 818.

- (55) Welsh, H.L., Crawford, M.F. and Locke, J.L. 1949. Phys. Rev. 76, 580.
- (56) Welsh, H.L., Crawford, M.F., McDonald, J.C.F. and Chisholm, D.A. 1951. Phys. Rev. 83, 1264.







